Spring 2020

Prediction of the Compressive Strength and Dynamic Modulus of Fiber Reinforced Concrete by Ultrasonic Pulse Velocity Measurement at Early Ages

Daniel A. Castillo Pereira

PREDICTION OF THE COMPRESSIVE STRENGTH AND DYNAMIC MODULUS OF FIBER REINFORCED CONCRETE BY ULTRASONIC PULSE VELOCITY MEASUREMENT AT EARLY AGES

by

DANIEL ANTONIO CASTILLO PEREIRA

(Under Direction of Saman Hedjazi)

ABSTRACT

This research investigates the relationship between early age ultrasonic pulse velocity and the compressive strength and dynamic modulus of steel, polypropylene, nylon, and glass fiber reinforced concrete. Previous studies prove that adding fibers to concrete alters the propagation of ultrasonic pulse velocity waves. Therefore, each type of fiber-reinforced concrete will have a unique relationship between ultrasonic pulse velocity and its compressive strength and dynamic modulus depending on fiber type, fiber volume fraction, water to cement ratio, and test age. To test this hypothesis, an experimental program comprising of one hundred eighty-nine 100 mm x 200 mm fiber reinforced concrete cylinders with varying fiber types, fiber volume fractions, and water-to-cement ratios will be tested using destructive and nondestructive test methods at the ages of 1, 3, 7, and 28 days. This research develops simple mathematical equations capable of predicting the compressive strength and dynamic modulus of different types of fiber-reinforced concrete based on early age ultrasonic pulse velocity. The equations for the prediction of the early age compressive strength of FRC had a coefficient of variation ranging from 6.4% to 14.6%. The equations for the prediction of the early age dynamic modulus of FRC had a coefficient of variation ranging from 3.3% to 9.2%. These equations can predict the compressive strength and dynamic modulus of multiple types of fiber reinforced concrete due to the incorporation of different fiber properties as variables in the equations.

INDEX WORDS: Nondestructive testing, Ultrasonic pulse velocity, Glass fiber reinforced concrete, Nylon fiber reinforced concrete, Polypropylene fiber reinforced concrete, Steel fiber reinforced concrete, Compressive Strength, Modulus of Elasticity, Early age properties of concrete, Fiber volume fraction

PREDICTION OF THE COMPRESSIVE STRENGTH AND DYNAMIC MODULUS OF FIBER REINFORCED CONCRETE BY ULTRASONIC PULSE VELOCITY MEASUREMENT AT EARLY AGES

by

DANIEL ANTONIO CASTILLO PEREIRA

B.S., Georgia Southern University, 2018

M.S., Georgia Southern University, 2020

A Thesis Submitted to the Graduate Faculty of Georgia Southern University in Partial Fulfillment of the Requirements for the Degree

MASTER OF SCIENCE

PREDICTION OF THE COMPRESSIVE STRENGTH AND DYNAMIC MODULUS OF FIBER REINFORCED CONCRETE BY ULTRASONIC PULSE VELOCITY MEASUREMENT AT EARLY AGES

by

DANIEL ANTONIO CASTILLO PEREIRA

Major Professor:	Saman Hedjazi
Committee:	David W. Scott
	Francisco Cubas

Electronic Version Approved:
May 2020

DEDICATION

This work is dedicated to my family and friends who have demonstrated their support and encouragement throughout the development of this report. A special sentiment of gratitude to Gundemaro and Lucia Castillo, my loving parents.

ACKNOWLEDGMENTS

I would like to thank my supervisor, Saman Hedjazi, for his guidance, encouragement, and advice throughout my time as a graduate student at Georgia Southern University.

TABLE OF CONTENTS

LIST OF TABLES

LIST OF FIGURES

CHAPTER 1

INTRODUCTION

Nondestructive testing (NDT) is a testing, analysis and research topic focusing on the examination of materials without destroying them. According to ACI 228.2R-13, NDT methods in concrete construction check for new construction quality, solve serious problems with new and old construction, assess the condition of aged concrete for rehabilitation, and ensure the quality of concrete repair. Using NDT methods to evaluate concrete structures is increasing because of the opportunity to perform quick and detailed evaluations of existing buildings, hardware and software improvements for data collection and analysis, specification of the NDT approaches for clear quality assurance, and the economic benefits of concrete evaluation compared with traditional approaches (Verma et al., 2013).

Traditional approaches for quality assurance of concrete construction consist of visual inspections, coring, which refers to drilling or cutting (destructive testing) a sample of the structure to perform standard tests, and surface sounding, which refers to striking an object and listening to the resulting sound characteristics. The information obtained from these traditional approaches is limited, and coring damages the existing structure and confines the information to the core location. NDT methods have the advantage of providing condition assessment without damaging the existing structure and at different locations. NDT methods can provide structural performance information such as dimensions, location of defects, degree of concrete consolidation, location and size of steel reinforcement, corrosion of reinforcement, strength of concrete, and dynamic modulus of concrete.

There are several NDT methods available for concrete evaluation, one of the most commonly used NDT methods is the Ultrasonic Pulse Velocity (UPV) (Wiciak, et al., 2017). It can assess concrete strength and dynamic modulus by measuring the velocity of an ultrasonic pulse which passes through a concrete structure. However, no unique relationship can be established between UPV and compressive strength or dynamic modulus to cover all concrete specimens because of the different mixture parameters such as cement type and content, aggregate type, size, and content, coarse to fine aggregate ratio, reinforcement

type and content, water to cement ratio, admixtures, and test age.

Many studies can be found in the literature using the UPV test method for evaluating the compressive strength or dynamic modulus of concrete (Lin, et al., 2007 and Khademi, et al., 2016). However, the majority of tests were performed to evaluate the 28 day (later age) compressive strength of concrete. In addition, the effect of concrete mixture parameters such as cement type and content, aggregate size and content, water to cement ratio, and silica fume on the UPV of concrete has also been studied. In contrast, the effect of mixture parameters such as the addition of different types and volume fractions of structural fibers on early age UPV, whether existing equations relating UPV to compressive strength of plain concrete are applicable for fiber reinforced concrete, and equations for predicting fiber reinforced concrete's (FRC) mechanical properties based on UPV at early ages (1 to 7 days) are not being studied and need to be investigated further.

In the present study one hundred eighty-nine 100 mm x 200 mm FRC cylindrical specimens were cast, cured, and tested for compressive strength, dynamic modulus, and ultrasonic pulse velocity. Mixture parameters such as fiber type, fiber volume fraction, water to cement ratio, and test age were investigated using the compression test machine, ultrasonic concrete tester, and resonance test gauge. This study develops a correlation between the mechanical properties and the ultrasonic pulse velocity of fiber reinforced concrete at the early ages of 3 and 7 days. Specifically, two sets of new equations will be proposed. The first set of equations predict the compressive strength of early age steel, polypropylene, nylon, and glass fiber reinforced concrete based on ultrasonic pulse velocity. The second set of equations predict the dynamic modulus of early age steel, polypropylene, nylon, and glass fiber reinforced concrete based on ultrasonic pulse velocity. The accuracy of these new equations was tested by measuring the coefficient of variation between the measured values and the predicted values from the proposed equations and existing equations found in the literature

CHAPTER 2

LITERATURE REVIEW

Plain Concrete

Concrete grades are defined by the composition of the concrete and the minimum strength the concrete should have after 28 days of initial construction. The grades of concrete are measured in MPa. Standard Grade Concrete ranges between 25 MPa and 45 MPa while, High Strength Concrete Grades range between 50 MPa and 70 MPa. On its own concrete has an excellent compressive strength, but when compared to other materials the tensile strength of concrete is relatively low. In addition, concrete has a low ductility and strength-to-weight ratio. To increase these and other properties of concrete different kinds of reinforcements such as structural fibers have been added to concrete.

Fiber Reinforced Concrete

The American Concrete Institute (ACI) defines Fiber Reinforced Concrete (FRC) as "concrete made primarily of hydraulic cements, aggregates, and discrete reinforcing fibers." ASTM C1116 classifies FRC into Type I steel fiber reinforced concrete, Type II glass fiber reinforced concrete, Type III synthetic fiber reinforced concrete, and Type IV natural fiber reinforced concrete.

Steel fibers are one of the most frequently used fibers for concrete reinforcement. They exist in various geometries due to their malleability and tri-axial stiffness. For example, steel fibers exist as hooked end, needles, and continuously deformed geometries (Nycon, 2020). Different geometries such as shape, length, and cross section influence the bond strength between the fiber and concrete. Hence, the geometry of the fibers can significantly affect the fresh and hardened properties of concrete (Dopko, 2018). Increasing the fiber's cross section and length increases the surface area for matrix bonding. In addition, twisting or bending the fibers provides better anchorage resulting in higher pull out strength, flexural strength, and toughness (Naaman, 2003; Kim et al., 2011; Soulioti et al., 2011).

Steel fibers have great tensile and flexural strength, so the use of steel fibers greatly enhances the mechanical properties of concrete. Several studies have concluded that increasing steel fiber volume increased the 28-day compressive, splitting tensile, and flexural strength of concrete (Song and Hwang, 2004; Afroughsabet et al., 2015 and Zheng et al., 2018). Similarly, the addition of steel fibers decreases brittleness, increases toughness, and controls crack initiation, growth and propagation (Pawade et al., 2011). However, the effect of structural fibers on the mechanical properties of concrete is dependent on mixture parameters such as fiber type, shape, aspect ratio, and volume fraction. Steel fibers can reduce the workability of concrete mixtures and cause fiber ball production at mid-to-high fiber volume fractions, resulting in a lack of homogeneity and reduction in concrete performance.

Steel fiber reinforced concrete (SFRC) has been used in a variety of applications due to its superior engineering properties such as highway and airfield pavements, hydraulic structures, and fiber shotcrete. Conversely, steel fibers should not be used for marine applications or other corrosion-prone conditions. Long term exposure to corrosion-prone conditions can result in steel fiber corrosion, resulting in a loss of steel strength, loss in reinforcing efficiency, and concrete deterioration (Kosa and Naaman, 1990 and Granju et al., 2004). Therefore, stainless steel fibers and brass-coated or zinc-coated steel fibers have been developed to limit corrosion. Steel fibers possess a density much higher than concrete and any other fiber. Consequently, steel fibers increase the unit weight of concrete, which can be a downside in lightweight applications. Moreover, since steel fibers have high densities, they would cost more than any other fiber for the same volume fraction.

Polypropylene fibers are commonly used to reinforce concrete mainly due to their availability, low cost, and chemical stability. Polypropylene fibers are non-magnetic, rust-free, alkali-resistant, and compatible with all concrete chemical admixtures. In addition, the hydrophobic surface of polypropylene fibers repels water, thus preventing the balling effect (Madhavi et al., 2014). The two most common types of polypropylene fibers are bundled (fibrillated) and single strand (monofilament) fibers, which can be found in micro or macro versions. Microfibers have a filament diameter less than 0.3 mm whereas macro

fibers have a filament diameter greater than 0.3 mm. Microfibers are used for plastic shrinkage control, impact protection, and fire anti-spalling. On the other hand, macro fibers may be used as a replacement for crack control mesh or as structural reinforcement in concrete or shotcrete (Fibermesh, 2016).

Polypropylene fibers have moderately low tensile and flexural strength. However, polypropylene fibers are extremely ductile and thus increase the toughness and impact resistance of concrete. Additionally, several studies have evaluated polypropylene fiber reinforced concrete (PFRC) performance. Numerous studies have found that the compressive, split tensile and flexural strength of concrete increases with the addition of polypropylene fibers up to 1.5% fiber volume fraction (Patel et al., 2012; Thirumurugan and Sivakumar, 2013; and Mohod, 2015). Polypropylene fibers increase entrapped air voids at 1.0% or higher fiber volume fractions, thereby decreasing concrete workability and creating difficulties when compacting the mixes (Madhavi et al., 2014). However, the workability can be improved by using high-range water reducing admixtures (Thirumurugan and Kumar, 2013). Lastly, the fibers can cause finishing issues.

Polypropylene fibers can be manufactured from recycled materials, which is an advantage over the majority of concrete fibers. Studies showed that recycled polypropylene fibers can produce fiber-reinforced concrete with the same mechanical properties as virgin polypropylene fibers (Yin et al., 2015 and Yin et al., 2016). In addition, polypropylene fibers have low melting points, and this property can be used to avoid spalling during fires in concrete structures. Throughout fires, the moisture within the concrete vaporizes and creates highly compressed gas. Simultaneously polypropylene fibers melt, thereby creating escape routes for the compressed gas, thus preventing spalling (Lee et al., 2012). Polypropylene fibers also have low densities, making them one of the most cost-effective fibers. This characteristic, combined with accessibility, chemical stability, and mechanical properties, has made polypropylene fibers one of the synthetic fibers most commonly used. Some general applications include roads, pavements, toppings, offshore structures, etc.

Nylon fibers are usually manufactured as micro or macro monofilament or ultra-fine monofilament

fibers. Microfibers have a length of 6 mm or less whereas macro fibers have a length of 13 mm or more. Monofilament fibers have a filament diameter of 0.038 mm while ultra-fine monofilament fibers have a filament diameter of 0.009 mm (Nycon, 2020). The flowability of self-compacted nylon fiber reinforced concrete decreases with an increase in fiber length and fiber volume fraction (Shanya, 2016). Nylon and polypropylene fibers have similar fiber/matrix bond strength, tensile strength and elastic modulus. However, they are chemically different (Dopko, 2018). In addition, nylon fibers can be manufactured from recycled materials and used as reinforcement in cement materials to improve tensile strength and fracture properties (Spadea et al., 2015).

Nylon fibers are hydrophilic, meaning they can absorb a small amount of water during mixing (ACI Report 544.1R-96, 2009). This characteristic can be favorable for the distribution of nylon fibers during mixing, but excess absorption at higher fiber volume fractions may adversely affect the workability of the mixtures (Song et al., 2015). Some researchers have tested the mechanical properties of nylon fiber reinforced concrete. Their experimental results revealed an increment of the compressive, splitting tensile, and flexural strength up to 1% fiber volume fraction (Nitin and Verma, 2016 and Subramanian et al., 2016). In addition, nylon fibers can decrease plastic shrinkage cracking, increase fracture energy, and post crack performance (Ozsar et al., 2017).

Nylon fibers are hydrophilic, and this characteristic is a disadvantage because it restricts them to applications with relatively small fiber volume fractions. Another disadvantage of nylon fibers is that they offer similar benefits to concrete as polypropylene fibers but are more costly because they have a slightly higher density. Nylon fibers are mainly used for shrinkage crack control, thermal crack control, impact resistance, shatter resistance, and abrasion resistance of concrete. Some common application includes architectural precast, stucco, commercial slab on grade, grouts, and mortar (Nycon, 2020).

Glass fibers are not used as widely as other fibers for concrete reinforcement, since their effects on concrete have not been researched as much as other fibers (Dopko, 2018). Glass fibers may be manufactured

in the form of a micro- or macro-mono-filament strands or as a roving glass spool. Researchers have mainly investigated silica and basalt glass fibers, but these types of glass fibers are limited in applications because they are non-alkali resistant. After being exposed to alkali and acid conditions, both fibers suffered total loss of strength and ductility. In contrast, both fibers displayed better resistance to salt solutions with a recorded loss of strength of forty percent (Wu et al., 2015). However, alkali resistant (AR) glass fibers can be produced by adding zirconium oxides in the fiber production process (Bentur and Mindess, 2006).

When using traditional mixing techniques to produce glass fiber reinforced concrete, high fiber volumes are difficult to achieve because glass fibers scatter unevenly and further mixing or an increase in water to cement ratio is needed (Bentur and Mindess, 2006). Due to excessive mixing, the long-term performance of glass fiber-reinforced concrete may be affected because the fibers might be destroyed (Johnston, 2001). Moreover, an increase in water to cement ratio affects the mechanical properties of concrete. Another disadvantage of glass fiber is that its density is higher than that of synthetic fibers, so they are more costly at the same volume fraction. However, at the correct fiber volume fraction, glass fiber can enhance the mechanical properties of concrete.

Alkali resistant silica glass fibers have relatively high tensile and flexural strength when compared to synthetic fibers. Researchers have investigated the performance of glass fiber-reinforced concrete considering fiber volume fractions ranging from 0.5% to 5% and have found that adding glass fibers to concrete can increase the compressive, split tensile, and flexural strength of concrete (Qureshi and Ahmed, 2013 and Bobde et al., 2018). In addition, glass fibers are known to control plastic shrinkage cracking, drying shrinkage cracking, lower the permeability of concrete, increase impact strength, and producing strong lightweight concrete (Nycon, 2020). Some common applications include precast concrete, residential slabs, fireplace surrounds, counter tops, and decorative panels.

Concrete Quality Tests

Concrete’s properties and behavior at an early age dramatically impact concrete’s long-term

efficiency. Therefore, to guarantee safety, long-term performance, and durability during accelerated construction schedules, an understanding of concrete behavior at an early age is needed. The early age of concrete is typically defined as the first few hours or days after casting concrete, which is marked by the setting and hardening processes (Nehdi and Soliman, 2011). The fluid phase of fresh concrete transitions into the hardened state, resulting in the formation of mechanical properties, heat release, and deformations due to the success of the hydration reactions (Pane and Hansen, 2002). The mechanical properties of early age concrete develop at different rates, depending on mixture proportions, w/c ratio, age, and curing conditions.

The gain in concrete compressive strength is rapid at an early age, with approximately 65% of the compressive strength reached in the first 7 days. Conversely, the gain in concrete elastic modulus is extremely rapid at an early age, with approximately 90% of the elastic modulus reached in the first 24 hours (Myers, 1999). This rapid, early gain in strength is directly linked to the increase of the gel/space ratio of calcium silicate hydrate (Neville, 2004). The researchers who have evaluated the early age mechanical properties of plain concrete typically use traditional compression tests. However, the effect of different types of structural fibers on the early age compressive strength and modulus of elasticity of fiber reinforced concrete at various fiber volume fractions need to be investigated further using nondestructive tests.

The compressive strength of cylindrical concrete specimens is determined experimentally in accordance to ASTM C39. Similarly, the static modulus of elasticity of concrete in compression is determined experimentally in accordance to ASTM C469. Both test methods use a testing machine that applies a compressive axial load to molded concrete cylinders or cores until failure occurs. This destructive method is considered antiquated for three reasons: its time consuming, the workload is high, and it requires several samples. The method is time consuming since concrete strength requirements are usually calculated after 28 days of curing because it takes concrete 28 days to achieve almost all its strength. The workload is high because thousands of pounds of rock, sand, water, admixture, and cement need to be lifted, measured, mixed, compacted, cured, and tested. Large quantities of samples are needed since the test method is

destructive and requires at least an average of two cylinders measured at the same age to comply with the standard. In addition, on site evaluation of aged concrete is limited because cores need to be extracted from the structure and the data obtained is confined to the core's location. Extracting too many cores will harm the integrity of the structure, so only a limited number of samples are collected. Consequently, the use of this method is inefficient for on-site maintenance evaluation.

The American Society of Civil Engineers' 2017 infrastructure report card ranked US infrastructure D+. Moreover, they estimate that the US needs to spend 4.5 trillion dollars by 2025 to inspect and give maintenance to the country's roads, bridges, dams, airports, schools, etc. The compression test machine is not suitable for on-site inspections. Therefore, non-destructive tests must be used to inspect and rehabilitate new and existing structures for safety, long term performance, and durability. However, nondestructive test methods need to be investigated further to ensure higher accuracy.

Particularly, the ultrasonic pulse velocity method is a popular technique used to predict the compressive strength and dynamic modulus of the elasticity of concrete. Knowing concrete's early age compressive strength and modulus of elasticity is important to ensure the long-term safety, quality, and durability of accelerated construction materials. Studies have been conducted and equations have been proposed to predict the early age mechanical properties or plain concrete based on ultrasonic pulse velocity (Popovics, et al., 1990 and Yoon, et al., 2017). However, the accuracy of predicting the early age mechanical properties of fiber reinforced concrete using existing equations based on the ultrasonic pulse velocity of plain concrete has not been investigated yet.

Ultrasonic Pulse Velocity

The standard test method for pulse velocity through concrete is reported in ASTM C597 and consists of calculating the time it takes for a pulse of vibrational energy to pass through a concrete component. Materials with high density, good quality, and continuity have high velocities, while materials with low density, several cracks, and voids have slow velocities. The ultrasonic pulse velocity can locate

voids, measure cracks, assess crack repairs, predict compressive strength, predict dynamic modulus of elasticity, evaluate the uniformity of concrete, and judge the general quality of concrete. The test method consists of an electrical transducer generating a longitudinal stress wave that travels through the concrete element being tested and is received by a second electrical transducer. The pulse velocity (V) is calculated using equation 1 by dividing the distance between the transducers (L) by the transit time (T).

$$V = \frac{L}{T} \tag{1}$$

The accuracy of the ultrasonic pulse velocity measurement depends on determining the exact distance between the transducers, measuring the transit time with the equipment accurately, and using the right amount of coupling agent to ensure a good contact between transducer and concrete surface (ASTM C597). The UPV measurement can be performed in three different configurations: direct transmission (opposite faces), semi-direct transmission (adjacent faces), and indirect/surface transmission (same face), from which the most accurate configuration is the direct transmission (Khademi et al., 2016). The testing configurations are shown in figure 1.

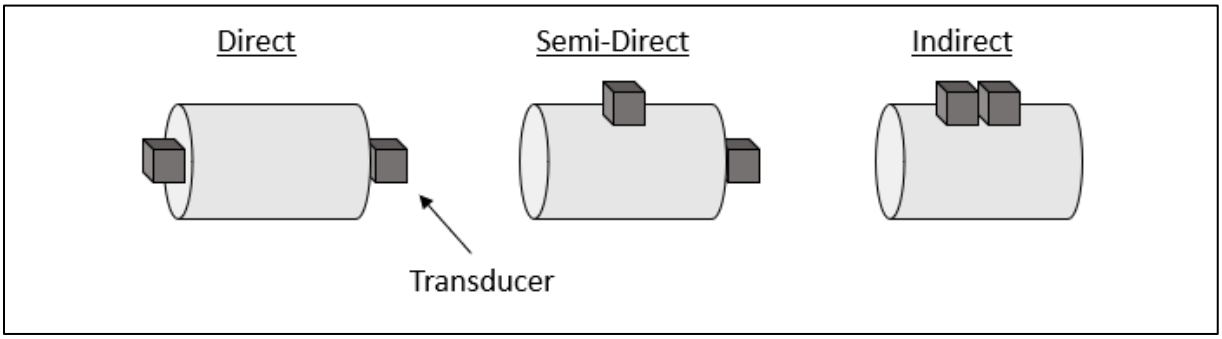

Figure 1: Ultrasonic pulse velocity testing configuration

Researchers have studied how different types, sizes, and dosages of coarse aggregate influence the measurement of ultrasonic pulse velocity and concluded that the ultrasonic pulse velocity is significantly affected by these parameters (Malhotra and Carino, 2004). In addition, ultrasonic pulse velocity and compressive strength measurements conducted at the age of 28 days revealed that the correlation between ultrasonic pulse velocity and compressive strength of concrete is significantly influenced by the coarse

aggregate content. (Al-Nu'man et al., 2016). For these reasons, when using the ultrasonic pulse velocity to predict concrete properties, the effect of coarse aggregates should be considered.

Investigators have studied concretes with different water to cement ratios and concluded that mixes with lower water to cement ratios have higher ultrasonic pulse velocities. Mixes with low water to cement ratios have high amounts of coarse aggregate and cement, thereby increasing the ultrasonic pulse velocity and strength (Ye et al., 2004 and Khademi et al., 2016). Therefore, the effect of water to cement ratio should be accounted for when using the ultrasonic pulse velocity test method to predict concrete properties.

Studies have tracked the development of ultrasonic pulse velocity based on curing age. It was reported that the rate of gain of ultrasonic pulse velocity was high during the early ages and then it slows down (Yoon et al., 2017). This increase in ultrasonic pulse velocity could be attributed to the hydration process and the increase of the gel/space ratio of calcium silicate hydrate during the setting and hardening process (Gebretsadik, 2013). That is why, existing equations for predicting the 28-day compressive strength of concrete based on 28-day ultrasonic pulse velocity are not applicable for early age concrete. Therefore, the effect of curing age should be considered when creating equations for predicting concrete properties.

Researchers have evaluated the effect of different curing temperatures on the ultrasonic pulse velocity measurement and concrete strength. Different temperatures represent concrete construction in different seasons. The investigators concluded that curing temperature influences the relationship between compressive strength and ultrasonic pulse velocity (Yoon et al., 2017).

Structural fibers can reduce the workability of concrete mixtures and cause fiber ball production at mid-to-high fiber volume fractions, resulting in a lack of homogeneity (ASTM C116). This lack of homogeneity results in the reduction of the ultrasonic pulse velocity. Additionally, the different materials that make up structural fibers have their own ultrasonic pulse velocity. Therefore, each type of fiber-reinforced concrete will have a unique relationship between concrete properties and ultrasonic pulse velocity.

Numerous researchers have investigated the relationship between the ultrasonic pulse velocity and the compressive strength of concrete. However, precise prediction of strength is difficult to obtain because the ultrasonic pulse velocity measurement is affected by numerous mixture parameters. The influence of water to cement ratio, temperature, coarse aggregate, shape and cement type have been investigated (Elvery and Ibrahim, 1976; Lin et al., 2007; Mahure et al., 2011). However, most existing equations focus on plain concrete and do not account for the addition of structural fibers (Naik et al., 2004 and Nash't et al., 2005). Although studies can be found relating steel fiber-reinforced concrete's ultrasonic pulse velocity to its compressive strength, not many studies can be found for polypropylene, nylon, and glass fiber reinforced concrete (Gebretsadik, 2013).

Additionally, many investigations focus on the relationship between 28-day ultrasonic pulse velocity and 28-day compressive strength of concrete (Lin et al., 2007 and Mahure et al., 2011). Some investigations can be found for early ages, but they are limited to plain concrete (Popovics et al., 1990 and Yoon et al., 2017). The simplest and most frequently used relationship between concrete compressive strength and ultrasonic pulse velocity is of the exponential form as shown in Table 1. However, some linear relationships have also been found in the literature. Table 1 lists equations found in the literature for prediction of concrete's compressive strength based on ultrasonic pulse velocity.

As it can be observed the equations listed in Table 1 are limited to specific mixture proportions. Therefore, a new empirical equation capable of predicting the early age compressive strength of different types of fiber-reinforced concrete at different fiber volume fractions and water-to-cement ratios is needed.

Table 1: Prediction of Concretes Compressive strength based on Ultrasonic Pulse Velocity

Reference	**Equation**	**Limitation**	**Equation No.**
Yoon et al., 2017	$f_c = 0.0098e^{3.412V}$	Early Age - 24 hour Super-Plasticizer C/S > 1	2
Popovics et al., 1990	$f_c = 0.0028e^{2.1V}$	Early Age - 7 day	3
Lin et al., 2007	$f_c = 0.00106e^{2.37V}$	Age - 28 day	4

		CA = 1000 kg/m^3	
Lin et al., 2007	$f_c = 0.00055e^{2.5V}$	Age - 28 day CA = 1100 kg/m^3	5
Elvery and Ibrahim, 1976	$f_c = 0.0012e^{2.27V}$	Ages of 3hr and over Temperature 0° to 60° C	6
Nash't et al., 2005	$f_c = 1.19e^{0.715V}$	Ages from 7 to 138 days Cubes	7
Jones, 1962	$f_c = 2.8e^{0.53V}$	Concrete slabs	8
Raouf and Ali, 1983	$f_c = 2.016e^{0.61V}$	Cubes	9
Naik et al., 2004	$f'_c = (-109.6 + 33V)$	Cylinder	10
Mahure et al., 2011	$f_c' = 9.502V - 18.89$	Age – 7 and 28 days Cubes M15 Grade	11
Mahure et al., 2011	$f_c' = 2.701V + 17.15$	Age – 7 and 28 days Cubes M20 Grade	12
Mahure et al., 2011	$f_c' = 4.104V + 19.23$	Age – 7 and 28 days Cubes M35 Grade	13
Kheder, 1999	$f_c' = 8.4 * 10^{-9}(V * 10^3)^{2.5921}$	Age – 7 to 90 days	14

Where f_c is compressive strength in MPa and V is ultrasonic pulse velocity in Km/sec

According to ASTM C597, the ultrasonic pulse velocity of concrete is related to its elastic properties and density. The relationship is shown below in equation 15. Where V is ultrasonic pulse velocity, E_d is dynamic modulus of elasticity, ρ is density, and v is the dynamic Poisson's ratio. Therefore, the dynamic modulus of elasticity of concrete can be found using equation 16. The dynamic modulus is the ratio of stress to strain under vibratory conditions and it is typically 20% to 40% higher than the static modulus. The relationship between dynamic and static modulus has been investigated, and empirical equations have been proposed such as equations 17 and 18 (Lyndon and Balendran, and BS8100 Part 2). Where E_c is static elastic modulus and E_d is dynamic elastic modulus.

$$V = \sqrt{\frac{E_d(1-v)}{\rho(1-2v)(1+v)}} \tag{15}$$

$$E_d = \frac{\rho V^2(1-2v)(1+v)}{(1-v)} \tag{16}$$

$$E_c = 0.83E_d \quad (17)$$

$$E_c = 1.25E_d - 19 \quad (18)$$

Resonance Test Gauge

From Hook's law, the modulus of elasticity is defined as the ratio of the stress to the strain. The modulus of elasticity indicates a material's resistance to being deformed and the stiffness of the material. The tension, compression, and bending test methods are used to calculate the static modulus whereas, nondestructive test methods measure the natural frequency of vibrations to determine the dynamic modulus.

ASTM C215 details the measurement of the fundamental transverse, longitudinal, and torsional resonant frequencies of concrete cubes and cylinders and how to calculate the dynamic Young's modulus of elasticity, dynamic modulus of rigidity, and dynamic Poisson's ratio. In the impact resonance method, a specimen is hit with a small hammer, and the response is measured by an accelerometer attached to the specimen. Three different fundamental resonant frequencies can be measured: longitudinal, transverse, and torsional. To determine these frequencies, different accelerometer attachment points and hammer strike locations, shown in figure 2, must be implemented depending on specimen geometry, and material properties. The dynamic Young's modulus of elasticity, E_d, from the fundamental transverse, and longitudinal frequencies are calculated using equation 19 and 20 respectively. The dynamic modulus of rigidity, G_d, is calculated using equation 21 and the dynamic Poisson's ratio, μ, is calculated using equation 22.

$$E_d = CMn^2 \quad (19)$$

$$E_d = DM(n')^2 \quad (20)$$

$$G_d = BM(n'')^2 \quad (21)$$

$$\mu = \frac{E_d}{2G_d} - 1 \quad (22)$$

Where M, is the mass of specimen in kilograms, n, is the fundamental transverse frequency in hertz,

n', is the fundamental longitudinal frequency in hertz, n'', is the fundamental torsional frequency in hertz, C, is equal to 1.6067 (L^3T/d^4), $N{\cdot}s^2$ ($kg{\cdot}m^2$) for a cylinder, D, is equal to 5.093 (L/d^2), $N{\cdot}s^2$ ($kg{\cdot}m^2$) for a cylinder, B, is equal to ($4LR/A$), $N{\cdot}s^2/$ ($kg{\cdot}m^2$) for a cylinder, R, is a shape factor equal to 1 for a cylinder, A, is the cross-sectional area of test specimen in m^2, L, is the length of specimen in meters, d, is the diameter of cylinder in meters, and T, is a correction factor that depends on the ratio of the radius of gyration, *K* (the radius of gyration for a cylinder is *d*/4), to the length of the specimen, *L*, and on Poisson's ratio. Values of *T* for Poisson's ratio of 1⁄6 are obtained from Table 1 in ASTM C 215.

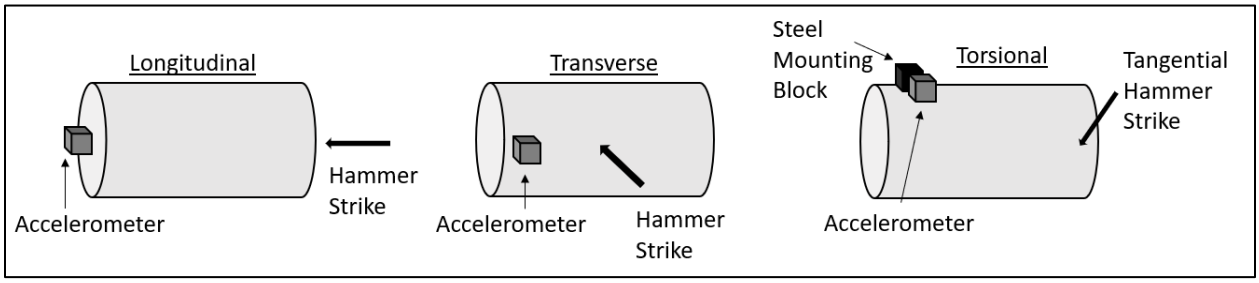

Figure 2: Longitudinal, Transverse, and Torsional Test Configurations

Researchers have successfully estimated the dynamic elastic constants of concrete cylinders based on the longitudinal resonance frequency (Kolluru et al., 2000). However, the researchers did not focus on the dynamic elastic constants of fiber reinforced concrete.

The accuracy of the resonance test gauge is dependent on several factors such as if the equipment selected to perform the test is working properly and is calibrated, the mixture proportions of the specimen being tested, and the ability of the operator to follow instructions and execute them. If the equipment and operator meet their expectations, the main factor influencing the resonance test gauge would be the mixture proportions. Young's modulus of concrete depends on aggregate content, aggregate type, water-to-cement ratio, cement content, admixtures etc. (Jurowski and Grzeszczyk, 2015). Additionally, the effect of structural fibers on the Young's modulus of concrete has also been investigated but mainly with destructive test methods (Abdullah et al, 2011; Gul et al, 2014; and Tharun et al, 2018). Therefore, the accuracy of nondestructive test methods such as the resonance test gauge to predict the dynamic elastic modulus of

concrete must investigated further especially for fiber-reinforced concrete since structural fibers could influence the resonance test gauge measurements.

Coefficient of Variation

An equation for calculating the coefficient of variation (COV) was used to understand the variability between the measured and predicted results. Where μ, is the mean measured value, n, is the number of data points, M_i, is the measured value for the i-th data point, and P_i, is the predicted value for the i-th data point. (Suksawang, et al., 2018).

$$COV = \frac{\sqrt{\frac{1}{n-1}\sum_{i=1}^{n}(M_i - P_i)^2}}{\mu} \tag{23}$$

$$\mu = \frac{\sum_{i=1}^{n} M_i}{n}$$

CHAPTER 3

EXPERIMENTAL PROGRAM

An experimental program designed and conducted in Georgia Southern University's materials laboratory was used to study the ultrasonic pulse velocity and mechanical properties of fiber reinforced concrete (FRC). The experimental program involved one hundred eighty-nine 100 mm x 200 mm FRC cylindrical specimens with different combinations of fiber type, fiber volume fraction, and water to cement ratio while the cement type and coarse aggregate maximum size remained constant for all mixtures. After curing in water for 1, 3, 7, and 28 days the ultrasonic pulse velocity of each specimen was measured. The dynamic modulus and compressive strength of each specimen were measured after 3, 7, and 28 days of curing in water. The experimental program outline is shown in Table 2.

Table 2: Experimental Program Outline

Portland Cement	TYPE I/II
Coarse Aggregate Nominal Maximum Size	4.7625 mm (0.1875")
Fiber Types	Nylon, Polypropylene, Steel, and Glass
Fiber Volume Fraction (%)	0.5, 1.0, and 1.5
Water-Cement Ratio	0.40, 0.45, and 0.50
Specimen Geometry	Cylinder 100 mm x 200 mm (4" x 8")
Curing Time (days)	1, 3, 7, 28
Destructive Test	Compression Test Machine
Non-destructive Tests Performed	Ultrasonic Pulse Velocity and Resonance Test Gauge
Mechanical Properties Evaluated	Compressive Strength and Dynamic Modulus

Materials

The concrete in this study consists of QUIKRETE Portland Cement Type I/II, gravel with a maximum size of 4.7625 mm (0.1875"), sand, tap water from Georgia Southern University's materials laboratory, and steel, polypropylene, nylon, and glass fibers. The fiber properties are presented in Table 3. The tools used to produce the concrete in this study consist of a digital scale, shovels, scoops, buckets, metal mixing bowls, sampling pans, gloves, safety glasses, dust mask, laboratory mixer, cylinder molds,

tamping rods, mallets, vibrating table, finishing trowel, and curing tank. The materials are shown in figure 3 and 4.

Table 3: Fiber Properties (Nycon, 2019)

	Stainless Steel	**AR Glass Fiber**	**Virgin Nylon**	**Polypropylene**
Filament Diameter (d)	1.18 mm	0.014 mm	0.038 mm	1.52 mm
Fiber Length (l)	25.4 mm	13 mm	19 mm	19 mm
Density (ρ)	7800	2700	1150	910
Tensile Strength (τ)	1030 MPa	2000 MPa	300 MPa	410 MPa
Flexural Strength (σ)	203 GPa	77 GPa	2.8 GPa	5.6 GPa
Melting Point	1516 °C	1121 °C	225 °C	160 °C
Water absorption	Nil	< 1%	3% by Weight	Nil
Alkali resistance	High	High	High	Excellent
Corrosion Resistance	High	High	High	High

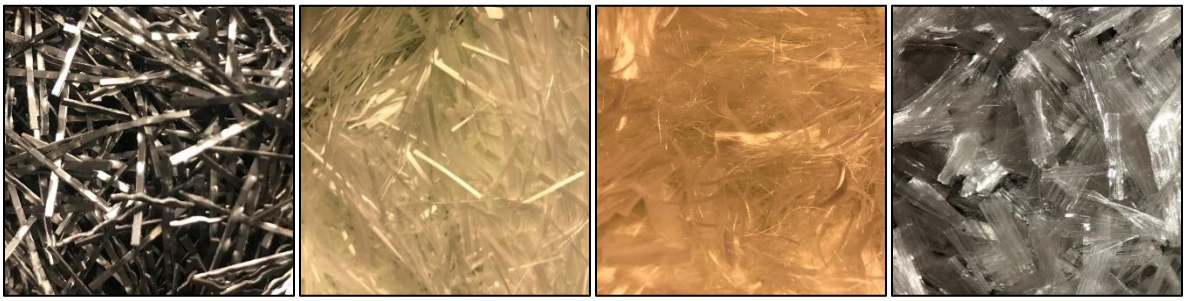

Figure 3: Stainless steel, AR glass, nylon, and polypropylene fibers

Figure 4: Portland cement, coarse aggregate, fine aggregate, and laboratory mixer

Mixture Proportions

Depending on the fiber type and intended application, structural fibers are applied to concrete at different dosages. Table 4 shows the fiber addition rates that manufacturers recommend, and Table 5 lists

studies that examined the performance of various types of fiber reinforced concrete at different fiber volume fractions. It can be observed that the fiber volume fraction range of 0% vol. to 1.0% vol. is applicable for all types of fibers considered in this investigation. In addition, having the same fiber volume fraction range allows for easy comparison between fibers. With regards to the selection of the water to cement ratio range, these studies investigated water to cement ratios varying from 0.35 to 0.55. Therefore, twenty-one mixes comprising of nylon, polypropylene, steel, and glass fibers at fiber volume fractions (Vf) of 0.5% vol., 0.75% vol., and 1.0% vol. and water to cement ratios 0.40, 0.45, and 0.50 were fabricated. Table 6 shows the different concrete mix proportions. Where, Vf, is fiber volume fraction, W/C, is water to cement ration, C, is cement, CA, is coarse aggregate, FA, is fine aggregate, and W, is water.

Table 4: Manufactures Recommended Fiber Addition Rates (Nycon, 2020)

Fiber Addition rate	Nylon	Polypropylene	Steel	Glass
Plastic shrinkage cracking	0.6 kg/m^3	0.9 kg/m^3	10 - 15 kg/m^3	0.3 - 0.6 kg/m^3
Structural Performance	-	-	15 - 80 kg/m^3	5 - 15 kg/m^3

Table 5: Common Fiber Volume Fraction Ranges

No.	Reference	Fiber Volume Fraction (Vf) Ranges			
		Steel	Glass	Nylon	Polypropylene
1	Gebretsadik, 2013	0 - 2%	-	-	-
2	Bobde et al., 2018	-	0 - 5%	-	-
3	Zheng et al., 2018	0 - 2%	-	-	-
4	Ramli and Hoe, 2010	-	0 - 2.4%	-	-
5	Nitin and Verma, 2016	-	-	0 – 1.5%	-
6	Pawade et al., 2011	0 – 1.5%	-	-	-
7	Mohod, 2015	-	-	-	0 – 2%
8	Suksawang et al., 2018	0 - 2%	-	-	0 - 2%

Table 6: Mixture Proportions

Fiber Type	Name	Vf (%)	W/C	C (kg/m3)	CA (kg/m3)	FA (kg/m3)	W (kg/m3)	Fiber (kg/m3)
Plain Concrete	Mix 1	0.00	0.40	503.3	709.7	986.5	201.3	0.0
Nylon	Mix 2	0.50	0.40	500.8	706.1	981.5	200.3	5.7
	Mix 3	0.75	0.40	499.5	704.3	979.1	199.8	8.5
	Mix 4	1.00	0.40	498.3	702.6	976.6	199.3	11.4
	Mix 5	0.75	0.45	487.3	687.1	955.0	219.3	8.5

	Mix 6	0.75	0.50	475.6	670.6	932.1	237.8	8.5
Polypropylene	Mix 7	0.50	0.40	500.8	706.1	981.5	200.3	4.5
	Mix 8	0.75	0.40	499.5	704.3	979.1	199.8	6.8
	Mix 9	1.00	0.40	498.3	702.6	976.6	199.3	9.1
	Mix 10	0.75	0.45	487.3	687.1	955.0	219.3	6.8
	Mix 11	0.75	0.50	475.6	670.6	932.1	237.8	6.8
Steel	Mix 12	0.50	0.40	500.8	706.1	981.5	200.3	39.0
	Mix 13	0.75	0.40	499.5	704.3	979.1	199.8	58.5
	Mix 14	1.00	0.40	498.3	702.6	976.6	199.3	78.0
	Mix 15	0.75	0.45	487.3	687.1	955.0	219.3	58.5
	Mix 16	0.75	0.50	475.6	670.6	932.1	237.8	58.5
Glass	Mix 17	0.50	0.40	500.8	706.1	981.5	200.3	13.5
	Mix 18	0.75	0.40	499.5	704.3	979.1	199.8	20.2
	Mix 19	1.00	0.40	498.3	702.6	976.6	199.3	27.0
	Mix 20	0.75	0.45	487.3	687.1	955.0	219.3	20.2
	Mix 21	0.75	0.50	475.6	670.6	932.1	237.8	20.2

Specimen Preparation

Twenty-one separate mixes (batches) were prepared by modifying variables such as fiber type, fiber volume fraction, and water to cement ratio. Nine specimens per mix were produced yielding a total of one hundred eighty-nine specimens. The one hundred eighty-nine specimens were categorized into five groups: the first group (Mix 1) had specimens with no fibers, the second group (Mix 2 – 6) had specimens with nylon fiber, the third group (Mix 7 – 11) had specimens with polypropylene fiber, the fourth group (Mix 12 – 16) had specimens with steel fibers, and the fifth group (Mix 17 – 21) had specimens with glass fiber. The concrete was mixed, poured, consolidated and cured in accordance to ASTM C192, illustrations can be found in figure 5. The concrete was mixed using a laboratory mixer. Then, the concrete was poured into 100 mm x 200 mm plastic molds. Subsequently, the concrete was consolidated by rodding and external vibration. Lastly, the cylinders were cured in water at room temperature after being demolded twenty-four hours from casting.

Figure 5: Consolidation, initial curing, removal of molds, and curing in water

Testing

After the specimens had cured in water for 1, 3, 7, and 28 days, nondestructive and destructive tests were carried out. The testing procedures began immediately after the curing process was completed and the specimens were removed from the curing tank, surface dried, and the ends of the cylinder surface ground and cleaned. The ultrasonic pulse velocity was measured at the ages of 1, 3, 7, and 28 days, and the dynamic modulus and compressive strength were measured at the ages of 3, 7, and 28 days. The dynamic modulus and compressive strength were not measured at the age of 1 day because of a small rate of gain in dynamic modulus and compressive strength. Furthermore, it was considered unnecessary to continue the testing procedures past 28 days because the focus of this study is on early ages, and concrete gains almost all its strength in 28 days, and test are normally implemented at the standard age of 28 days.

The ultrasonic pulse velocity of each specimen was determined according to ASTM C597. The UPV was determined by the direct transmission configuration where the transmitter and receiver transducers are placed directly opposite of each other on parallel surfaces. The transmitting transducer generated pulses of longitudinal stress waves, and after traveling through the concrete the pulses were received and converted to electrical energy by the receiving transducer. The pulse velocity (V) was calculated by dividing the length (L) of the specimen by the transit time (T). Sufficient coupling agent and pressure were applied to the transducers to ensure stable transit times. The ultrasonic pulse velocity of each specimen was calculated in kilometers per second, an average of four transit time measurements was used. Additionally, the test results

of three specimens per mix assessed the ultrasonic pulse velocity of each mix at each age. Figure 6 shows the process of ultrasonic pulse velocity measurement.

Figure 6: Ultrasonic pulse velocity hardware, calibration, testing, and data collection

The dynamic modulus of each specimen was determined according to ASTM C215 using the resonance test gauge. The dynamic modulus was determined by the impact resonance method using the longitudinal configuration, where the accelerometer and the hammer strike are directly opposite of each other on parallel surfaces. The accelerometer was attached to the specimen using a small amount of coupling grease. The vibrational energy was generated by a small hammer, which according to Olson Instruments Inc. specialist is intended for smaller specimens (100 mm x 200 mm) and received by the accelerometer. The time domain acceleration data was processed using the Fast Fourier Transform (FFT), which allows for the resonant frequency peak to be identified. The software calculated automatically the dynamic modulus of each specimen using equation 20 based on the longitudinal frequency, mass, geometry and dimension of the specimen. When defining the dynamic modulus of each specimen in GPa, an average of three longitudinal frequency measurements was used. Additionally, the test results of three specimens per mix assessed the dynamic modulus of each mix at each age. Figure 7 shows the process to obtain the longitudinal frequency using the resonance test gauge.

Figure 7: Resonance test gauge hardware, accelerometer, longitudinal frequency testing, and data collection

The compressive strength of all cylinders was tested according to ASTM C39 using a compression test machine. The compressive strength of each cylindrical specimen was calculated automatically by the compression test machine by dividing the maximum load obtained during the test by the cross-sectional area of the specimen. To determine the compressive strength of each mix at each age, an average of three cylinder compression tests per mix was used. Figure 8 illustrates the process of determining the compressive strength of cylindrical concrete specimens.

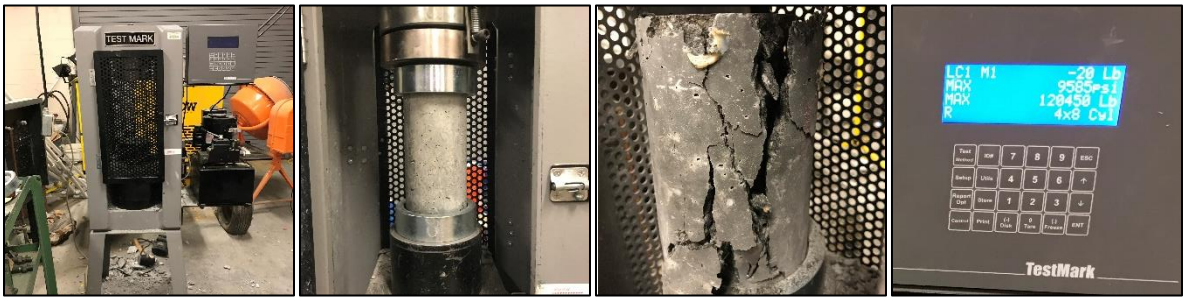

Figure 8: Testing machine, placing the specimen, crack in the specimen, and data collection

CHAPTER 4

ANALYSIS/RESULTS

Nylon Fiber Reinforced Concrete (NFRC)

The development of the ultrasonic pulse velocity, compressive strength, and dynamic modulus of five mixes containing nylon fibers at different fiber volume fractions and water to cement ratios is reported in Figure 9, 10, and 11 respectively.

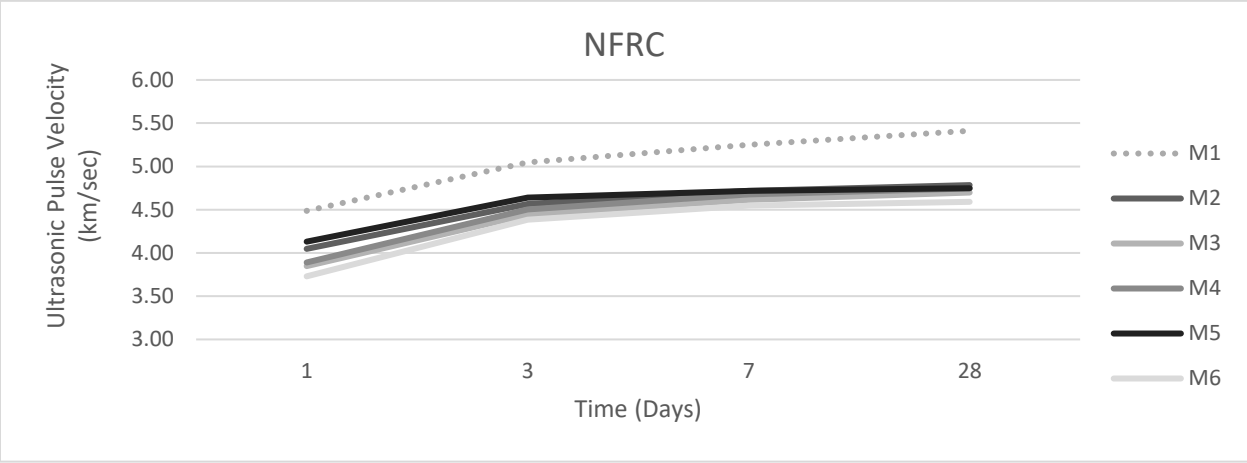

Figure 9: NFRC's ultrasonic pulse velocity vs time

It can be observed in Figure 9, 14, 19, and 24 that the gain in ultrasonic pulse velocity is rapid during early ages for all mixes. This happened because water causes the hardening of concrete through the process of hydration. The hydration process is faster at early ages because there are many unhydrated compounds and empty spaces in the cement paste. Therefore, as time passes, the empty spaces are filled with calcium silicate hydrate, thus increasing the ultrasonic pulse velocity. In addition, the ultrasonic pulse velocity is influenced by the fiber type. As mentioned in Table 3, nylon fibers absorb water, which reduces the mix's water-to-cement ratio. Due to water absorbing nylon fibers, M2-M6's workability was reduced, resulting in poor concrete homogeneity and the lowest ultrasonic pulse velocity measurements when compared to the other fibers shown in Figures 14, 19, and 24. In other words, when the water-to-cement

ratio is too low the workability of FRC is reduced resulting in low ultrasonic pulse velocity measurements. M5 achieved the highest ultrasonic pulse velocity from the mixes containing nylon fibers because it had a moderate amount of fibers (0.75% vol.) and a moderate water to cement ratio (0.45) that compensated for water-absorbing nylon fibers.

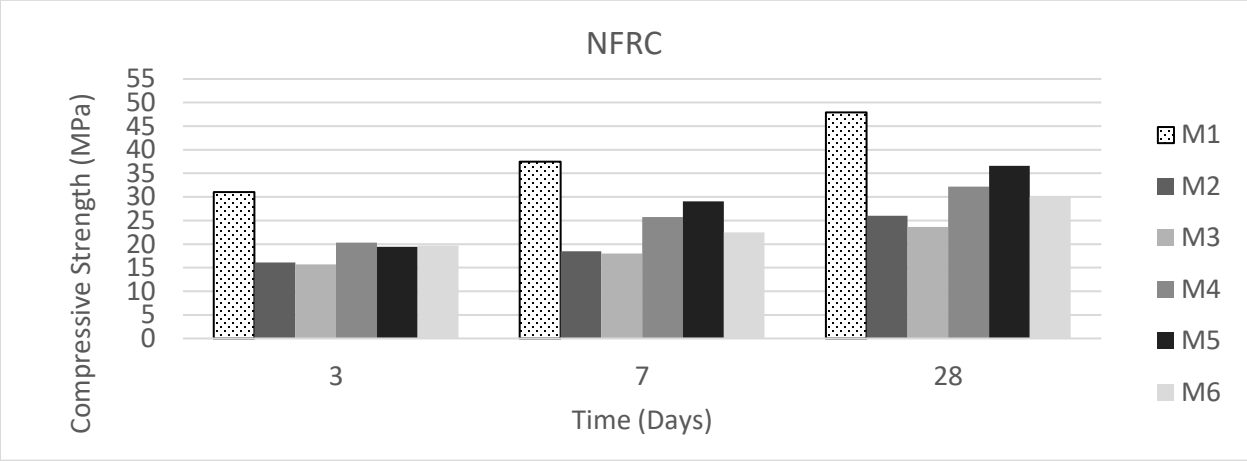

Figure 10: NFRC's compressive strength vs time

In Figure 10, 15, 20, and 25 approximately 70% of concrete's compressive strength is achieved in the first 7 days for all mixes. This is attributed to the hydration process. In addition, fibers provide internal reinforcement due to the fiber-bridging effect. The fiber-bridging constitutive law describes the relationship between the bridging stress transferred across a crack and the opening of this crack (Yang et al., 2008). As shown in Table 3, nylon fibers possess the lowest tensile and flexural strength when compared to the other fibers in this study. Therefore, NFRC obtained the lowest compressive strength when compared to the other types of FRC shown in Figures 15, 20, and 25. Another factor affecting the compressive strength of NFRC was the lack of concrete homogeneity, due to the reduced workability/water-to-cement ratio caused by water absorbing nylon fibers. As expected M5 attained the highest compressive strength from the mixes containing nylon fibers because it had the highest ultrasonic pulse velocity thanks to its moderate fiber volume fraction (0.75% vol.) and moderate water to cement ratio (0.45), which compensated for water absorbing nylon fibers. Therefore, nylon fibers should be added in small dosages, and the amount of water

that they absorb should be accounted for in order to ensure NFRC's performance.

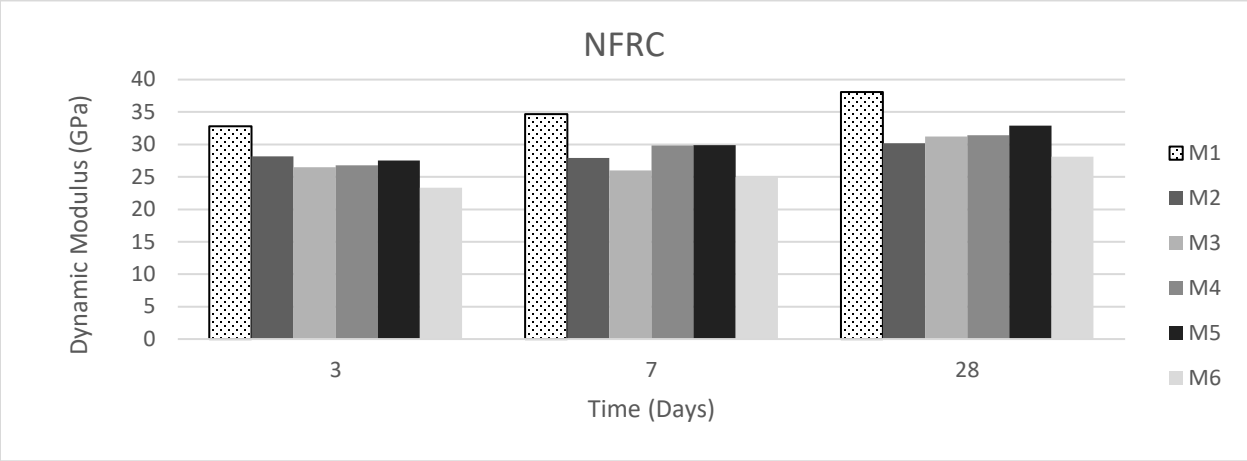

Figure 11: NFRC's dynamic modulus vs time

Figure 11, 16, 21, and 26 show that the development of the dynamic modulus of concrete is extremely rapid. Approximately 85% of the dynamic modulus was achieved after 3 days for all mixes. This happened because concrete becomes stiff very quickly due to the hydration process. It can also be observed that there isn't a big difference between the dynamic modulus of one mix from another because the change in fiber volume fraction does not affect the dynamic modulus as much as the compressive strength. On the other hand, increasing the water to cement ratio significantly decreases the dynamic modulus because there is less coarse aggregate and cement in the mix. When compared to the other fibers in this study, nylon fibers possess the lowest tensile and flexural strength. Therefore, NFRC obtained the lowest dynamic modulus when compared to the other types of FRC shown in Figures 16, 21, and 26. Moreover, NFRC was expected to have the lowest dynamic modulus because the modulus of elasticity of concrete is frequently expressed in terms of compressive strength, and NFRC had the lowest compressive strength. M5 obtained the highest dynamic modulus from the mixes containing nylon fibers because its fiber volume fraction was high enough to increase the bridging stress across a crack, and low enough to avoid workability issues.

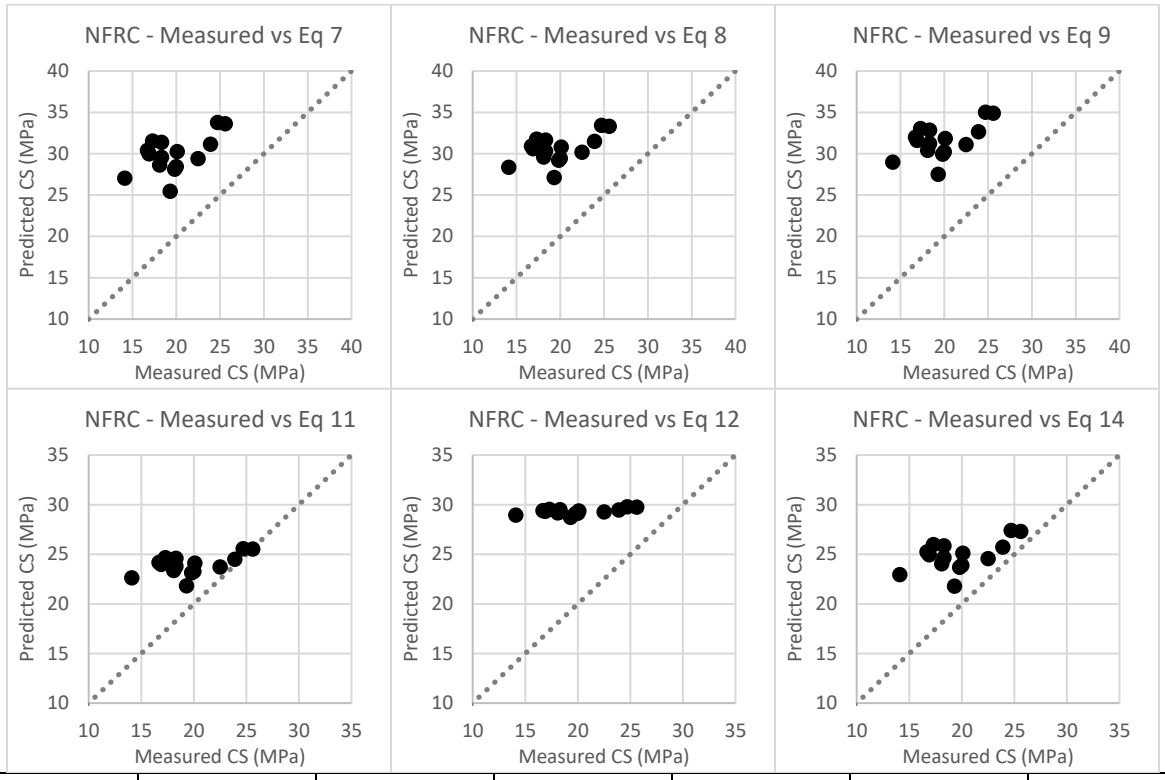

Equation #	7	8	9	11	12	14
COV	59.5%	62.7%	67.9%	30.5%	56.9%	34.5%

Figure 12: NFRC's 3-day measured compressive strength vs predicted compressive strength from existing equations found in the literature

Figure 12 compares NFRC's 3-day measured compressive strength to the predicted compressive strength from equations shown in Table 1. The coefficient of variation (COV) calculated using equation 23 is used to understand the variability between measured and predicted results. When the data points form a 45-degree line a perfect correlation is achieved. The data points below the 45-degree line represent conservative deviations while the data points above this line represent unconservative deviations. The six equations selected had the lowest COV's from all the equations in Table 1. However, all the equations used overestimated NFRC's compressive strength with the lowest COV's belonging to equation 11 and 14. The reason why these equations overestimated NFRC's compressive strength is because they are limited to specific mix proportions which do not include nylon fibers. Therefore, fiber type is an important parameter that should be included when creating an equation to predict the mechanical properties of fiber reinforced

concrete.

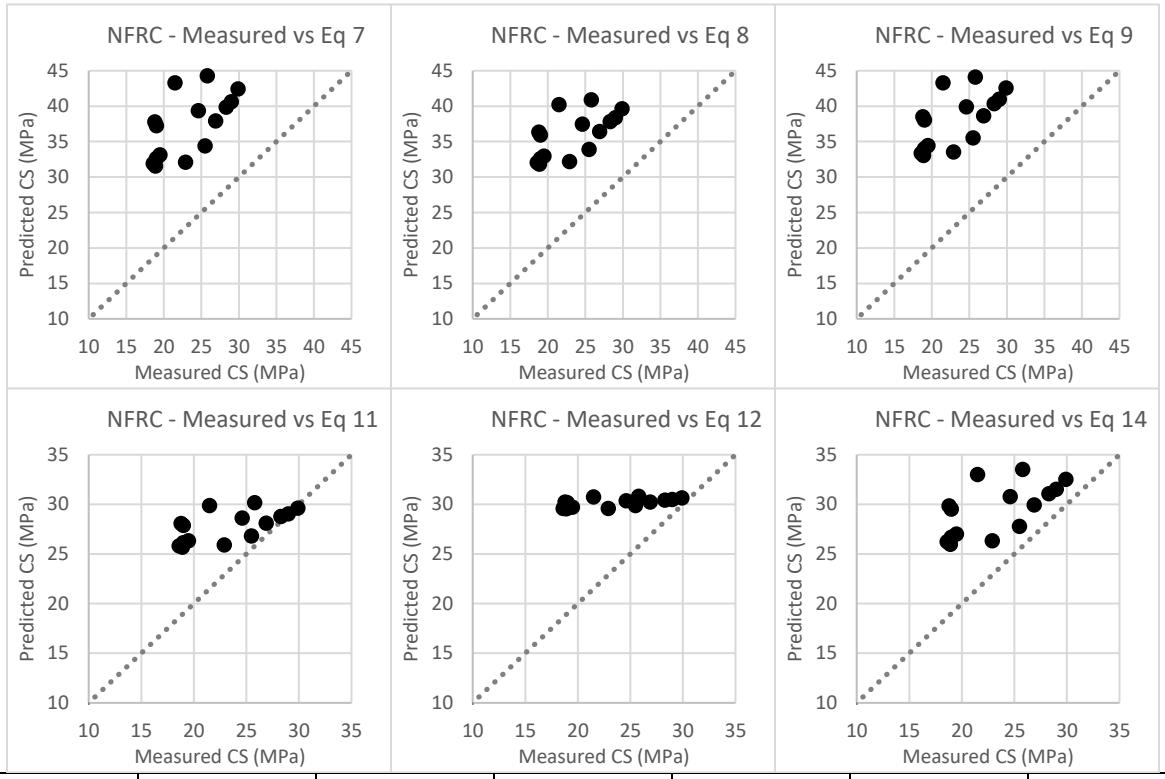

Equation #	7	8	9	11	12	14
COV	64.6%	58.3%	67.7%	25.1%	35.1%	31.1%

Figure 13: NFRC's 7-day measured compressive strength vs predicted compressive strength from existing equations found in the literature

Figure 13 shows the comparison between NFRC's 7-day measured compressive strength to the predicted compressive strength using equations from Table 1. All the equations have high COV's because of their limitations and none of them can accurately predict NFRC's 7-day compressive strength. Equation 11 provides the best estimation of NFRC's compressive strength. However, it is still overestimating NFRC's compressive strength. The COV's from 3-day NFRC are different from the COV's of 7-day NFRC. This revels that the test age is an important parameter that has not being accounted for by the equations. Test age is therefore an important parameter that should be included when creating an equation to predict the mechanical properties of fiber reinforced concrete.

Polypropylene Fiber Reinforced Concrete (PFRC)

This section covers the development of the ultrasonic pulse velocity, compressive strength, and dynamic modulus of five mixes containing polypropylene fibers at different fiber volume fractions and water to cement ratios.

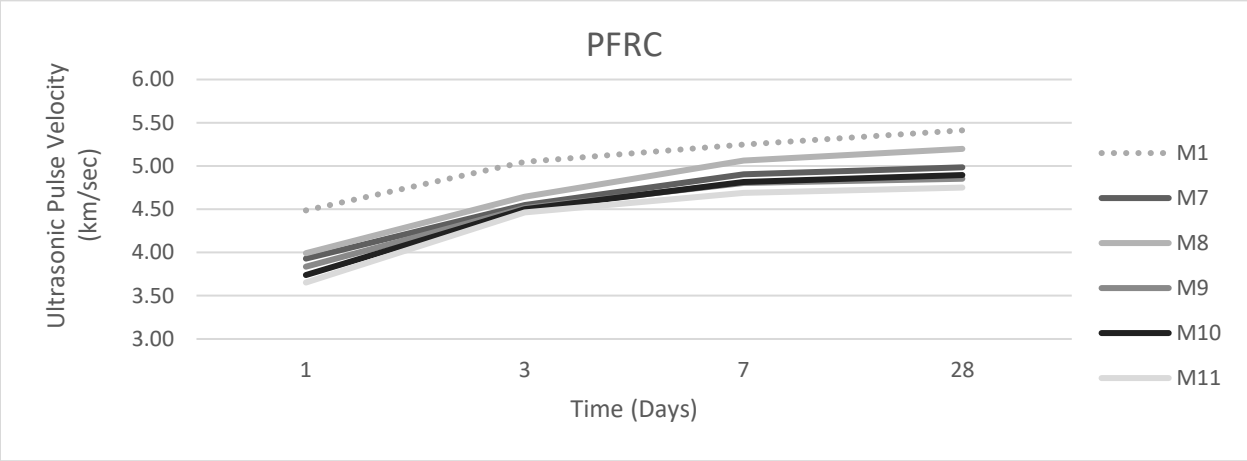

Figure 14: PFRC's ultrasonic pulse velocity vs time

Figure 14 shows how PFRC's ultrasonic pulse velocity increases over time. It can be observed that the gain in ultrasonic pulse velocity is faster during early ages. This is attributed to the hydration process. As stated in Table 3, polypropylene fibers do not absorb water. Therefore, PFRC's water-to-cement ratio/workability was not reduced, resulting in homogenous concrete and higher ultrasonic pulse velocity measurements than NFRC and GFRC, which contain water absorbing fibers that affect workability. In addition, it can be seen in Figures 9, 14, 19, and 24 that the mixes with water-to-cement ratio that are too high (M6, M11, M16, and M21) always have the lowest ultrasonic pulse velocity measurements because they have the lowest amounts of coarse aggregate and cement. M8 obtained the highest ultrasonic pulse velocity from the mixes containing polypropylene fibers because it possessed a moderate fiber volume fraction (0.75% vol) and a low water to cement ratio (0.4). A moderate fiber volume fraction prevents workability issues and a low water to cement ratio means more coarse aggregate and cement content resulting in higher ultrasonic pulse velocity.

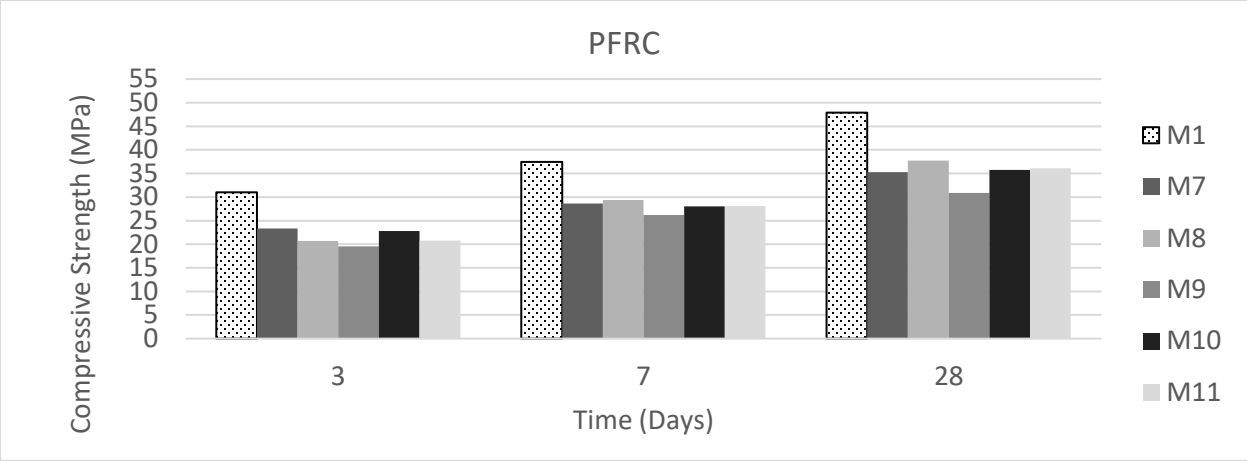

Figure 15: PFRC's compressive strength vs time

Figure 15 displays PFRC's compressive strength at different ages. Roughly 75% of PFRC's compressive strength was achieved after 7-days due to the hydration process. Moreover, the fiber bridging effect serves as internal reinforcement. As stated in Table 3, polypropylene fibers possess a relatively high tensile and flexural strength when compared to nylon fibers. In addition, polypropylene fibers have a hydrophobic surface that repels water thus reducing fiber ball production which generates lack of homogeneity (Madhavi et al., 2014). For these reason the compressive strength of PFRC is higher than the compressive strength of NFRC and GFRC shown in figures 10 and 20. M8 obtained the highest compressive strength from the mixes containing polypropylene fibers because of its moderate fiber volume fraction (0.75% vol) and low water to cement ratio (0.40). Having a moderate fiber volume fraction provides internal reinforcement and maintaining a low water-to-cement ratio allows for a higher coarse aggregate and cement content. The lowest compressive strength was obtained by M9 because it had a high fiber volume fraction (1.0% vol.) and a low water-to-cement ratio (0.40) resulting in the worst workability and homogeneity.

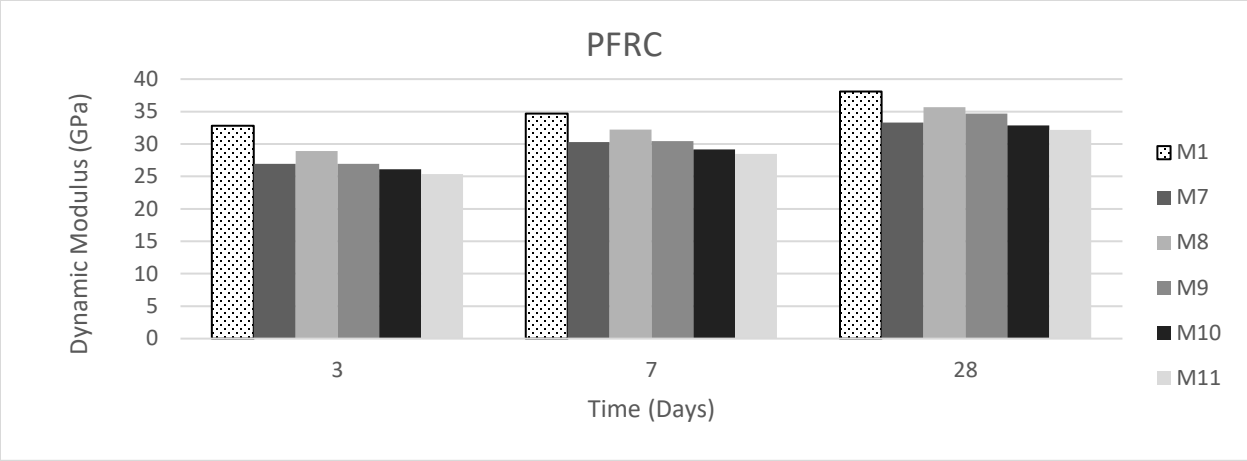

Figure 16: PFRC's dynamic modulus vs time

Figure 16 presents the dynamic modulus of five different PFRC mixes. It can be observed that approximately 80% of PFRC's dynamic modulus was achieved in the first 3 days. This is attributed to the early setting and hardening of concrete. In addition, there is no big difference between the dynamic modulus of one mixture to another, because fibers do not significantly affect the stiffness of concrete. This trend can be observed in figures 11, 21, and 26. The tensile and flexural strength of polypropylene fibers is only higher than nylon's. However, the dynamic modulus of PFRC is higher than NFRC's and very similar to GFRC's as shown in figures 11 and 26 respectively. Based on the tensile and flexural strength of glass fibers shown in Table 3, GFRC should have a higher dynamic modulus than PFRC. However, glass fibers absorb water and scatter unevenly which reduces the workability and affects the homogeneity of concrete. On the other hand, polypropylene fibers have hydrophobic surfaces thus generating homogenous concrete, resulting in a high dynamic modulus despite of its relatively low tensile and flexural strength. M8 obtained the highest dynamic modulus of elasticity from the mixes containing polypropylene fibers, which was expected due to its mix proportions and high compressive strength.

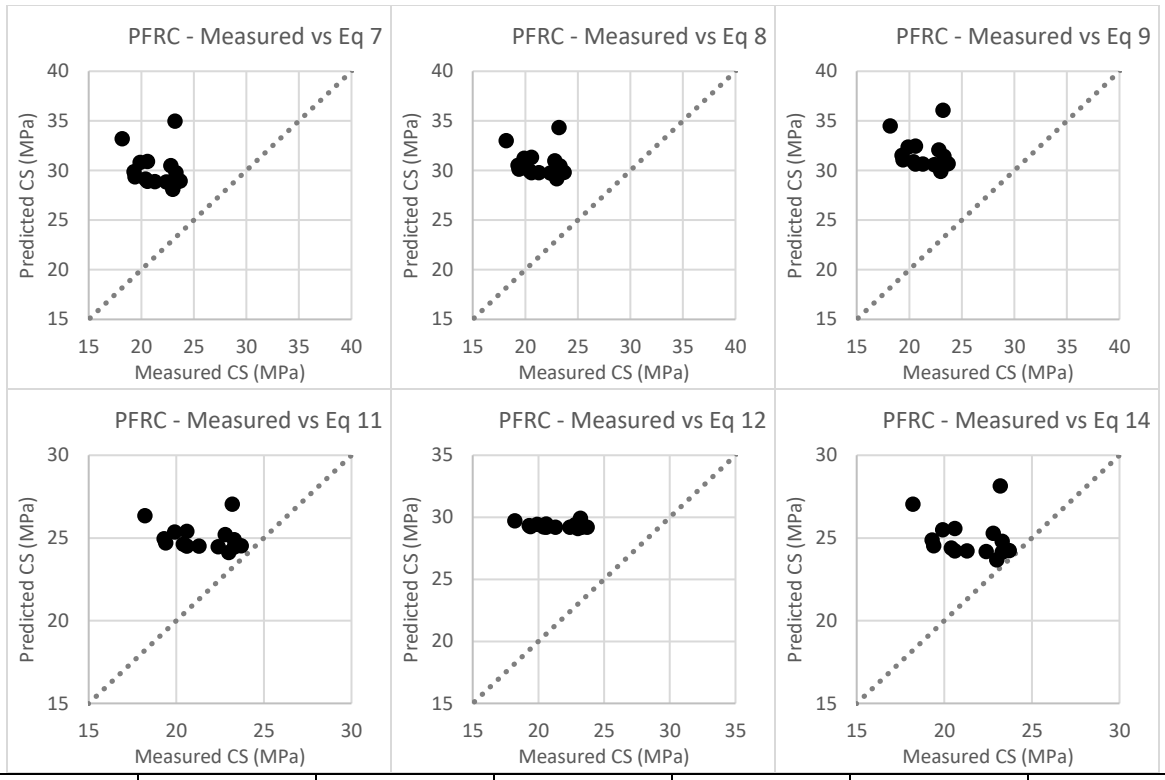

Equation #	7	8	9	11	12	14
COV	43.7%	46.1%	51.1%	19.8%	39.2%	20.4%

Figure 17: PFRC's 3-day measured compressive strength vs predicted compressive strength from existing equations found in the literature

Figure 17 compares PFRC's 3-day measured compressive strength to the predicted compressive strength using equations from Table 1. The six equations selected had the lowest COV from all equations in Table 1. All equations used for comparison overestimate PFRC's compressive strength. The lowest COV's were obtained by equation 11 and 14. The COV's of equation 11 and 14 a reasonable for PFRC but unreasonable for NFRC. This shows two that none of these equations can be used for both NFRC and PFRC. Therefore, in addition to considering different fiber types such as polypropylene, a single equation capable of predicting the mechanical properties of more than one type of FRC should be considered when creating an equation to predict the mechanical properties of fiber reinforced concrete.

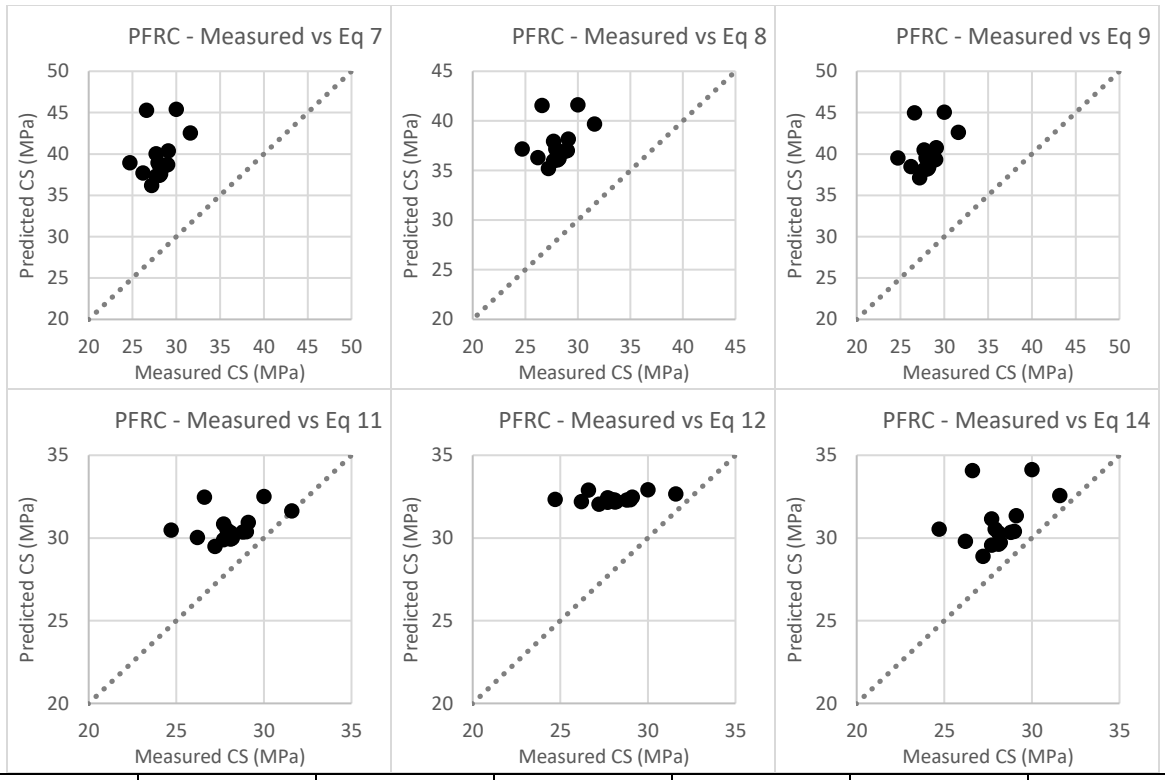

Equation #	7	8	9	11	12	14
COV	43.5%	35.9%	45.1%	11.1%	16.9%	12.3%

Figure 18: PFRC's 7-day measured compressive strength vs predicted compressive strength from existing equations found in the literature

Figure 18 compares PFRC's 7-day measured compressive strength to the predicted compressive strength from equations in Table 1. All of the equations used to predict the compressive strength of PFRC are overestimating its compressive strength. Equations 11, 12, and 14 however show good COV's when predicting the compressive strength of 7-day PFRC. Just as when comparing Figure 12 to Figure 13, the COV's from 3-day PFRC are different from the COV's of 7-day PFRC. This confirms that test age is a major parameter when predicting the mechanical properties of concrete. It also opens the possibility of a single equation capable of adjusting not only for fiber type but also for test age.

Steel Fiber Reinforced Concrete (SFRC)

This section comprises of the development of the ultrasonic pulse velocity, compressive strength, and dynamic modulus of five mixes containing steel fibers at different fiber volume fractions and water to

cement ratios.

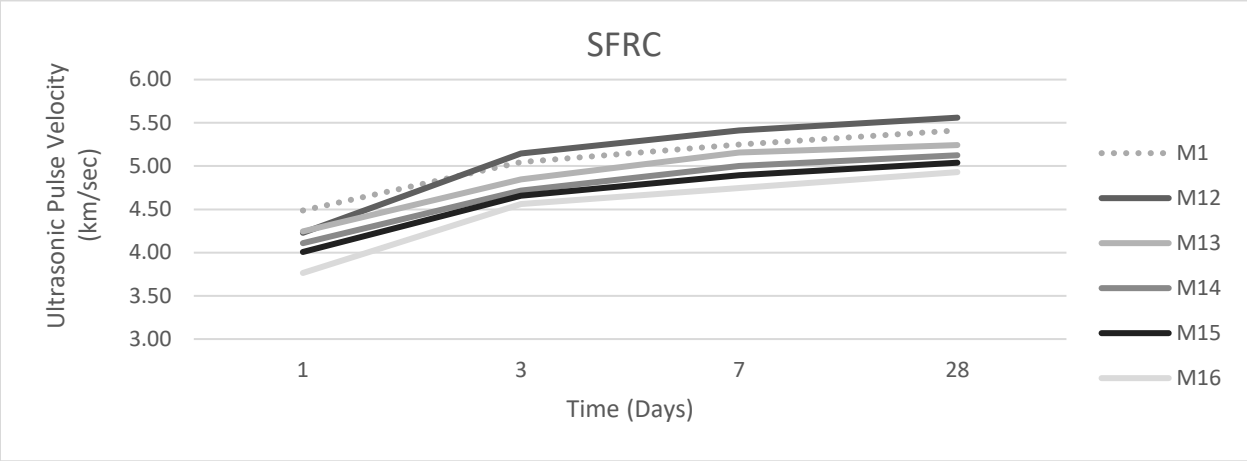

Figure 19: SFRC's ultrasonic pulse velocity vs time

Figure 19 shows the development of SFRC's ultrasonic pulse velocity over time. The development of the ultrasonic pulse velocity was rapid during the early ages due to the hydration process. The ultrasonic pulse velocity depends on the density of the material being tested. Compared with the other fibers, steel fibers have the highest density as shown in Table 3. In addition, the ultrasonic pulse velocity of steel is almost twice as fast as concretes. Therefore, SFRC had the highest ultrasonic pulse velocity out of all types of fiber reinforced concrete's which can be seen when comparing Figure 19 to Figures 9, 14, and 24. However, high volumes of steel fibers can reduce the workability, resulting in poor concrete homogeneity and low ultrasonic pulse velocity. That is why M14 had a lower ultrasonic pulse velocity than M13 and M12. The highest ultrasonic pulse velocity was obtained by M12 because it contained a low fiber volume fraction (0.5% vol.) and a low water to cement ratio (0.40) therefore the workability was not reduced as much as other mixes with higher fiber volume fractions. The lowest ultrasonic pulse velocity was achieved by M16 because it had a high water to cement ratio (0.50). Having a water to cement ratio that is too high results in low ultrasonic pulse velocity as can be seen in Figure 9, 14, and 24.

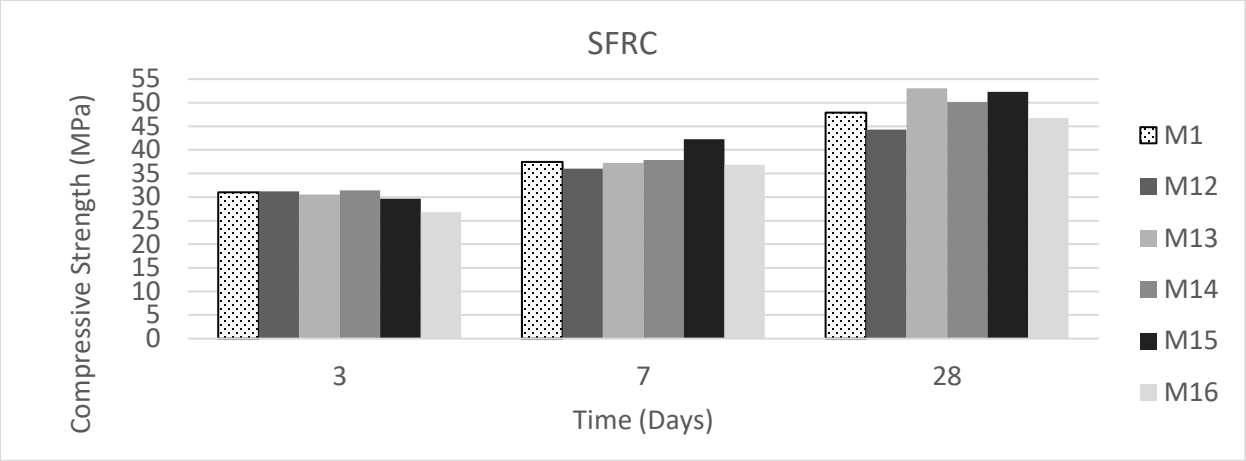

Figure 20: SFRC's compressive strength vs time

Figure 20 displays the development of SFRC's compressive strength over time. Due to the hydration process approximately 75% of SFRC's compressive strength was achieved in the first 7 days. In addition, according to Table 3, steel fibers have a high tensile strength and the highest flexural strength from all fibers under investigation. Therefore, steel fibers provide the highest capability to resist the bridging stress transferred across a crack. For this reason, SFRC obtained the highest compressive strength at all ages when compared to NFRC, PFRC, and GFRC shown in figures 10, 15, and 20 respectively. M13 obtained the highest compressive strength from the mixes containing steel fiber because it contained a moderate fiber volume fraction (0.75% vol.) and a low water to cement ratio (0.40). The moderate fiber volume fraction provided sufficient capability to withstand the bridging stress transferred across a crack without reducing the workability too much, and the low water-to-cement ratio allowed a high content of coarse aggregate and cement.

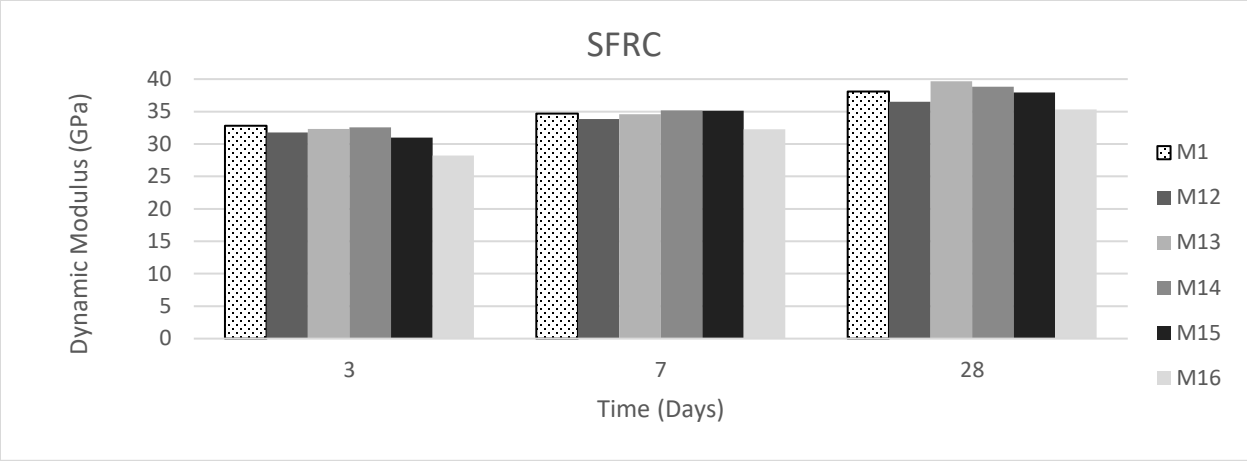

Figure 21: SFRC's dynamic modulus vs time

Figure 21 shows the dynamic modulus of SFRC at different ages. Roughly 80% of SFRC's dynamic modulus was achieved in the first 3 days due to concrete hardening throughout the hydration process. Once again, it can be observed that there is not a very big difference between the dynamic modulus of one mixture with another. Similarly, the mixture with the highest water-to-cement ratio showed the lowest dynamic modulus. SFRC obtained the highest dynamic modulus out of all types of fiber reinforced concrete due to the high tensile and flexural strength of steel fibers. Moreover, SFRC was expected to have the highest dynamic modulus because it had the greatest compressive strength. The highest dynamic modulus from the mixes containing steel fibers was obtained by M12 because it contained a moderate fiber volume fraction (0.75% vol.) and low water to cement ratio (0.40). The moderate fiber volume fraction provided a high fiber bridging effect without a significant decrease in workability. In addition, a low water-to-cement ration permitted high contents of coarse aggregate and cement. The lowest dynamic modulus belonged to M16 which had the highest water-to-cement ratio.

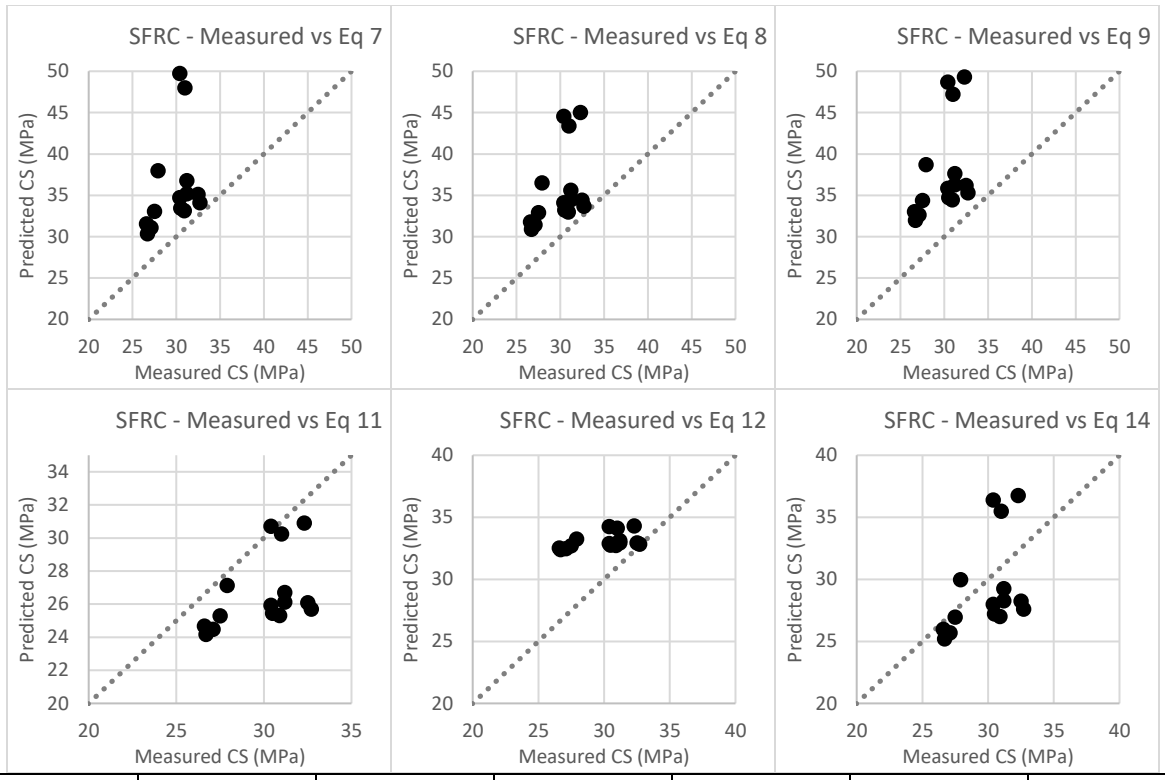

Equation #	7	8	9	11	12	14
COV	31.8%	24.3%	32.2%	13.8%	12.7%	11.8%

Figure 22: SFRC's 3-day measured compressive strength vs predicted compressive strength from existing equations found in the literature

Figure 22 compares SFRC's 3-day measured compressive strength to the predicted compressive from the equations in Table 1. Equation 7, 8, 9, and 12 overestimated SFRC's compressive strength. On the other hand, equation 11 and 14 underestimated SFRC's compressive strength. The COV's of equations 11, 12, and 14 are good for 3-days SFRC. These equations didn't obtain COV's as good as these one's for 3-day NFRC or PFRC as shown in figures 12 and 17. Reaffirming the importance of fiber type and test age. In addition, the data points of NFRC's and PFRC's scatter plots were not as dispersed as the data points of SFRC's scatter plots. This shows not only the effect of fiber type, but also the effect of fiber volume fraction on the ultrasonic pulse velocity. When the ultrasonic pulse velocity is altered by fiber type and fiber volume fraction the precision of the existing equation is inadequate. Therefore, fiber type and fiber volume fraction are important parameters that should be incorporated when creating an equation to predict the mechanical properties of fiber reinforced concrete.

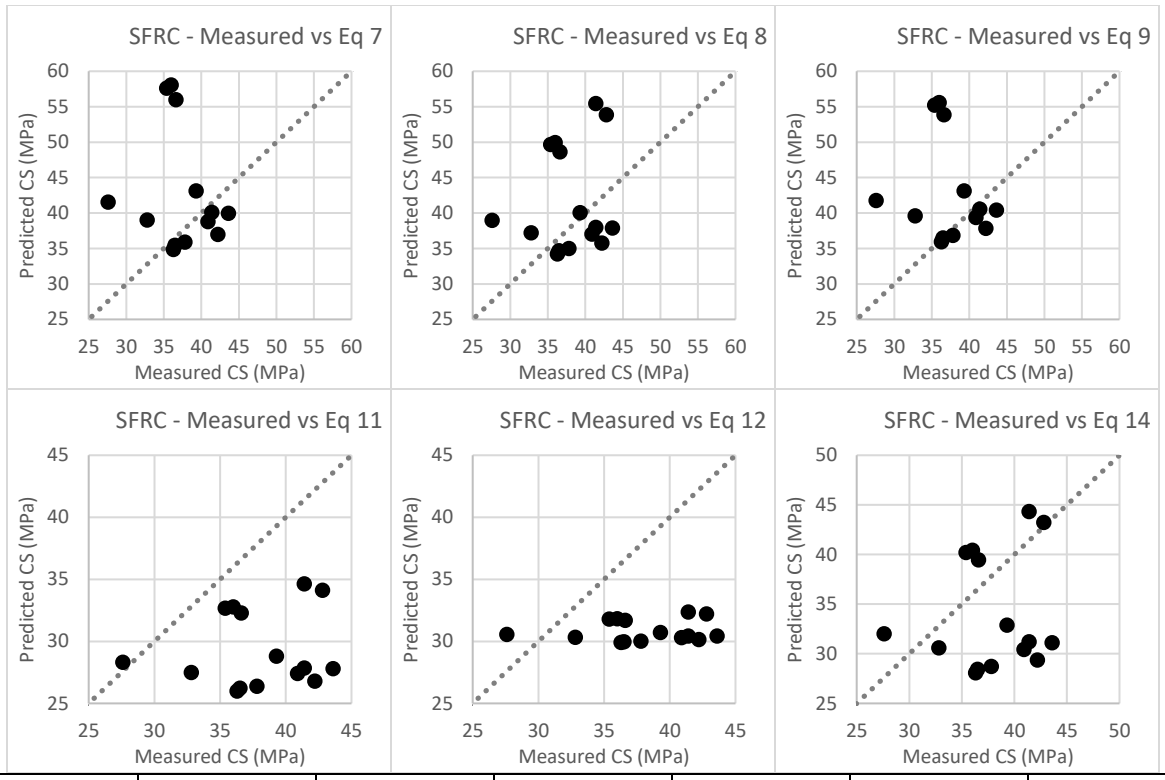

Equation #	7	8	9	11	12	14
COV	36.9%	23.6%	32.5%	27.1%	22.6%	20.8%

Figure 23: SFRC's 7-day measured compressive strength vs predicted compressive strength from existing equations found in the literature

Figure 23 shows the comparison between SFRC's 7-day compressive strength and the predicted compressive strength from the equations in Table 1. The data points in figure 23 are more dispersed than those in figure 22 and all other scatter plots. This occurred because steel fibers have a higher density than nylon, polypropylene, and glass fibers. Therefore, steel fibers have a greater effect on the ultrasonic pulse velocity. These scatter plots demonstrate the importance of taking into consideration the effect of fiber type, fiber volume fraction, and test age when creating an equation for predicting the mechanical properties of fiber reinforced concrete.

Glass Fiber Reinforced Concrete (GFRC)

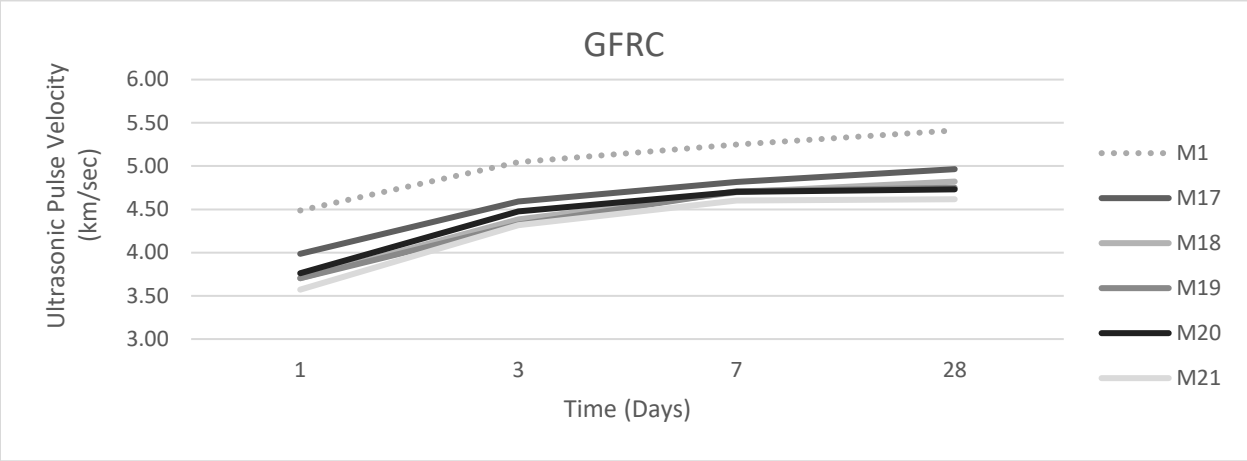

Figure 24: GFRC's ultrasonic pulse velocity vs time

Figure 24 displays the development of GFRC's ultrasonic pulse velocity over time. In the early ages the hydration process leads to a rapid increase in the ultrasonic pulse velocity. Glass fibers absorb a small amount of water which reduces the mix's water-to-cement ratio, workability, and homogeneity. However, as stated in Table 3, glass fibers do not absorb as much water as nylon fibers. For this reason, GFRC's ultrasonic pulse velocity is higher than NFRC's. The use of fibers reduces the workability of concrete causing fiber ball production (balling) generating lack of homogeneity, specially at high fiber volume fractions as can be seen in Figure 9, 14, 19, and 24. The highest ultrasonic pulse velocity from the mixes containing glass fiber was achieved by M17 which had a low fiber volume fraction (0.5% vol.) and a low water to cement ratio (0.40). M17 had good workability due to the low amount of fibers, and the coarse aggregate and cement content were high due to the low water-to-cement ratio resulting in high ultrasonic pulse velocity.

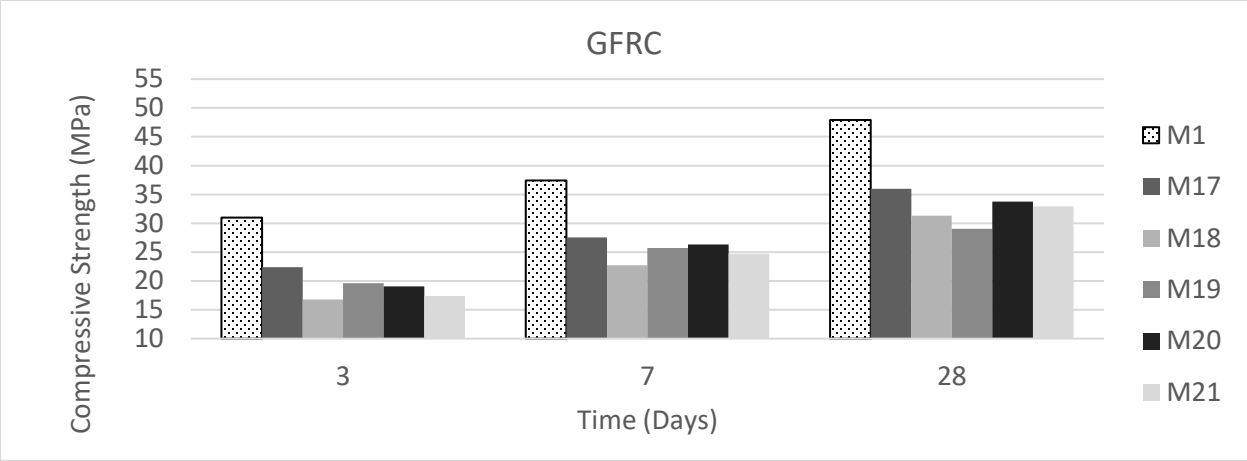

Figure 25: GFRC's compressive strength vs time

Figure 25 exhibits the development of GFRC's compressive strength over time. Nearly, 65% of GFRC's compressive strength was achieved in the first 7 days. This is attributed to the hydration process and the internal reinforcement provided by the fibers. According to Table 3, glass fibers have the highest tensile strength of all fibers under investigation and a flexural strength greater than NFRC and PFRC. However, GFRC obtained a lower compressive strength than PFRC because glass fibers absorb water and scatter unevenly. Therefore, further mixing is required which may destroy the fibers (Johnston, 2001). The highest compressive strength from the mixes containing glass fiber was obtained by M17 because it had a low fiber volume fraction (0.5% vol.) and a low water to cement ratio (0.40). The low fiber volume fraction offered reinforcement without affecting too much the workability, and the low water-to-cement ratio allowed for more coarse aggregate and cement content.

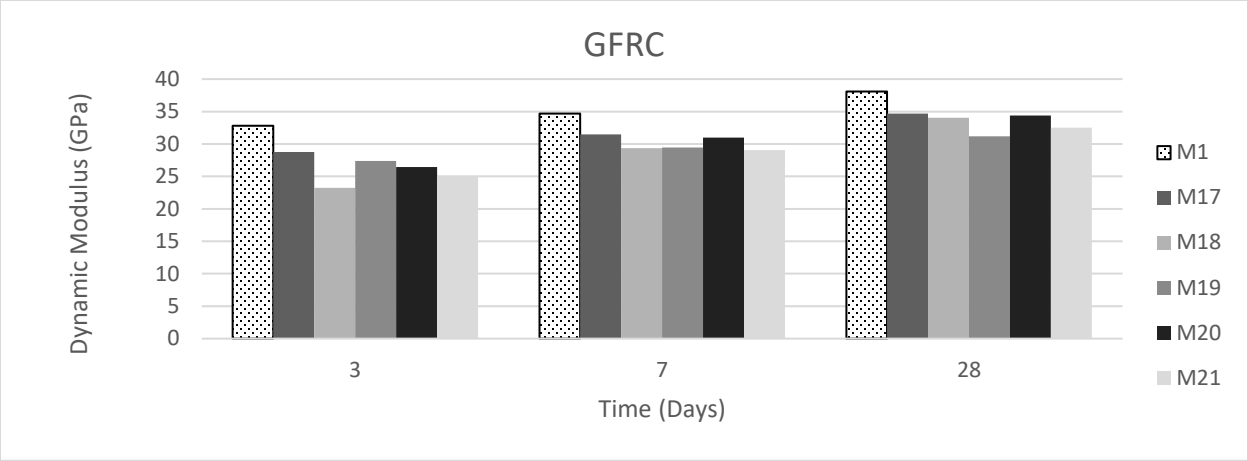

Figure 26: GFRC's dynamic modulus vs time

Figure 26 illustrates the increase of the dynamic modulus of GFRC over a period of 28 days. Roughly 80% of GFRC's dynamic modulus was achieved in the first 3 days due to the hydration process. The dynamic modulus of GFRC was stunt due to reduced workability. As stated in Table 3, glass fibers absorb water which reduced the water-to-cement ratio/workability of M17-M21. Reduced workability leads to limited fiber bridging effect and concrete homogeneity. Therefore, even though glass fibers had the highest tensile strength and a high flexural strength its dynamic modulus was not very high when compared to PFRC or SFRC. To enhance the performance of GFRC admixtures should be used to improve the dispersion of glass fibers and the workability of the cement paste. M17 obtained the highest dynamic modulus due to its low fiber volume fraction (0.5% vol) and low water to cement ratio (0.40). The lowest dynamic modulus was obtained by M19 due to its high fiber volume fraction (1.0% vol.) and low water to cement ratio (0.40). Having a high fiber content meant that more water would be absorbed by the glass fibers, which would reduce concrete workability and homogeneity. In addition, having a low water-to-cement ratio to begin with made matters worse.

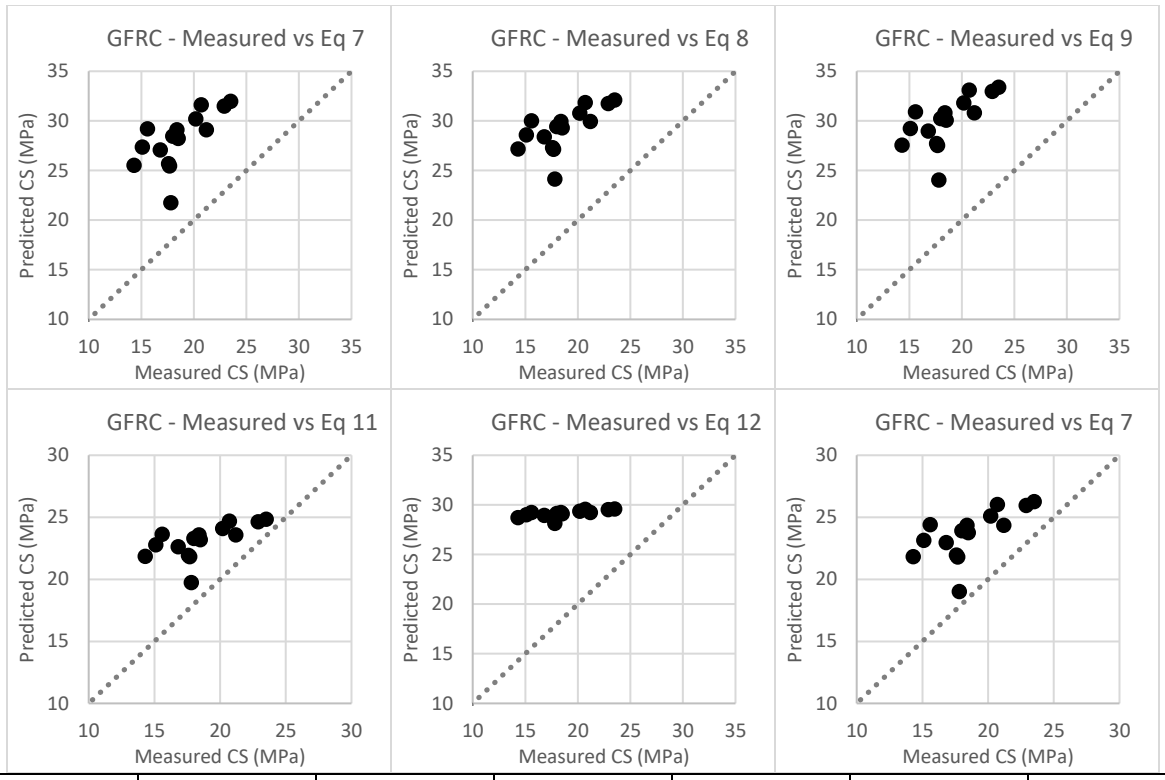

Equation #	7	8	9	11	12	14
COV	54.9%	60.4%	64.7%	27.8%	60.2%	30.6%

Figure 27: GFRC's 3-day measured compressive strength vs predicted compressive strength from existing equations found in the literature

Figure 27 compares GFRC's 3-day measured compressive strength to the predicted compressive strength from equations in Table 1. All of the equations used overestimated GFRC's compressive strength due to mixture parameters and have high COV's. In addition to mixture parameters such as fiber type, fiber volume fraction, and test age the prediction of the mechanical properties of fiber reinforced concrete is affected by the water-to-cement ratio. Having a high water to cement ratio typically results in a low ultrasonic pulse velocity. On the other hand, having a low water-to-cement ratio typically results in a high ultrasonic pulse velocity, unless the water-to-cement ratio is low enough to cause problems with workability and homogeneity. Therefore, the water-to-cement ratio is an important parameter that should be considered when creating an equation to predict the mechanical properties of FRC.

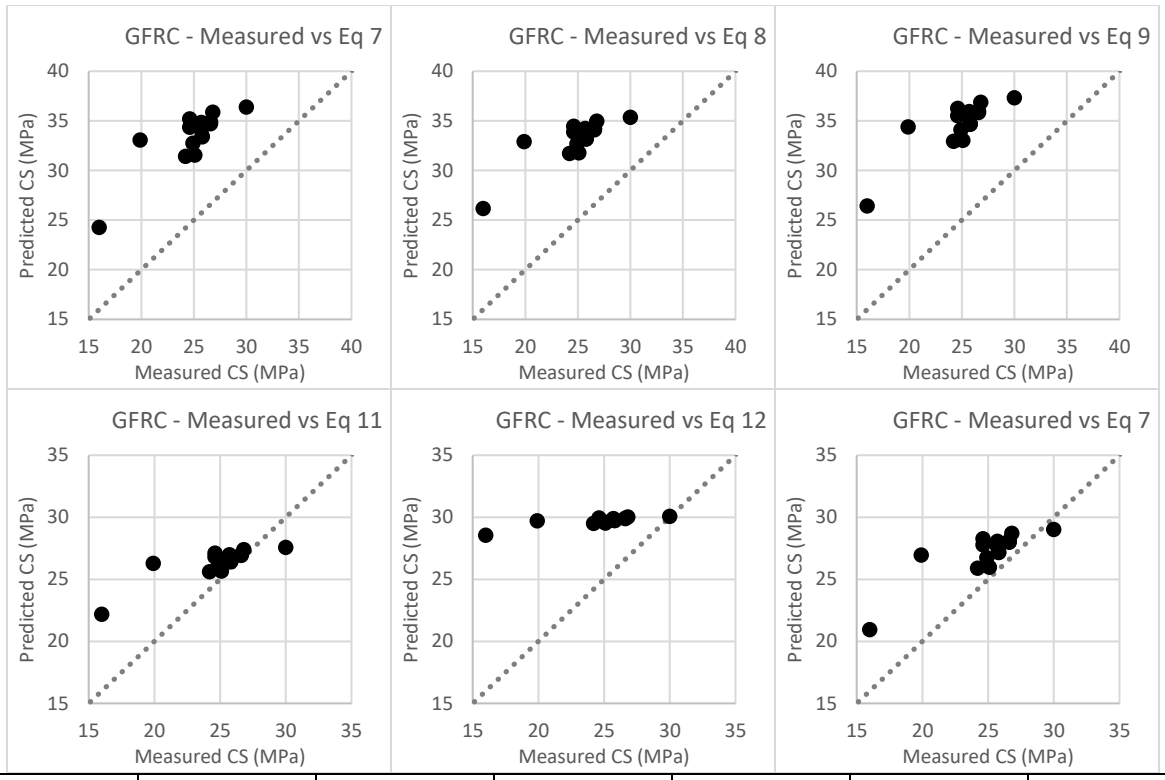

Equation #	7	8	9	11	12	14
COV	36.7%	35.8%	41.9%	11.7%	24.3%	12.7%

Figure 28: GFRC's 7-day measured compressive strength vs predicted compressive strength from existing equations found in the literature

Figure 28 compares GFRC's 7 day measured compressive strength to the predicted compressive strength from the equation in Table 1. Equations 7, 8, 9, and 12 significantly overestimate NFRC's compressive strength. On the other hand, equations 11 and 14 slightly overestimate NFRC's compressive strength resulting in good COV's. Having considered the application of the equations in Table 1 to predict FRC's early age compressive strength, it was determined that there is no single equation capable of predicting the compressive strength of different types of FRC's at different ages while taking into account the effect of fiber volume fraction and water-to-cement ratio.

Proposed Equations

The proposed equation 24 can predict the compressive strength of 3-day and 7-day SFRC, GFRC, PFRC, and NFRC with fiber volume fractions ranging from 0.5% vol. to 1% vol. and water to cement ratio

ranging from 0.40 to 0.50. The development trend with hydration time is the same for both the early age compressive strength and early age ultrasonic pulse velocity, where compressive strength and ultrasonic pulse velocity increase exponentially over time. Therefore, the prediction of FRC's compressive strength at early ages based on ultrasonic pulse velocity is expressed using an exponential relationship (Khademi et al., 2016). The proposed equations can predict the compressive strength of multiple fiber reinforced concrete types, due to the incorporation of different fiber properties as variables in the equations. No other equations have been found in the literature capable of predicting the compressive strength of multiple types of fiber reinforced concrete with different mixture parameters accurately. In addition, the test age is a variable in the equation making it applicable for both 3-day or 7-day prediction of the compressive strength. The proposed equations showed great results for all types of fiber reinforced concrete considered in this study. The proposed equations for prediction of SFRC, GFRC, PFRC, and NFRC compressive strength are shown below.

For G, P, and NFRC $$f_c = \alpha e^{0.59*V} \quad (24a)$$

For SFRC $$f_c = \alpha e^{0.15*V} \quad (24b)$$

Where f_c is compressive strength (MPa), V is the ultrasonic pulse velocity (km/sec) and α is calculated using equation 25 and fiber properties in Table 3. G, P, and NFRC were grouped together because they had a low density, while SFRC was left alone because it had a high density.

For G, P, and NFRC $$\alpha = 0.4\left(\frac{\sigma}{l/d}\right) + t^{0.1(\frac{\tau}{\rho})} + 0.3 \quad (25a)$$

For SFRC $$\alpha = 1.2\left(\frac{\sigma}{l/d}\right) + t^{6.8(\frac{\tau}{\rho})} + 0.3 \quad (25b)$$

Where σ is fiber flexural strength (GPa), l is fiber length, d is fiber diameter, t is the age (days), τ is fiber tensile strength (MPa), and ρ is fiber density (kg/m^3).

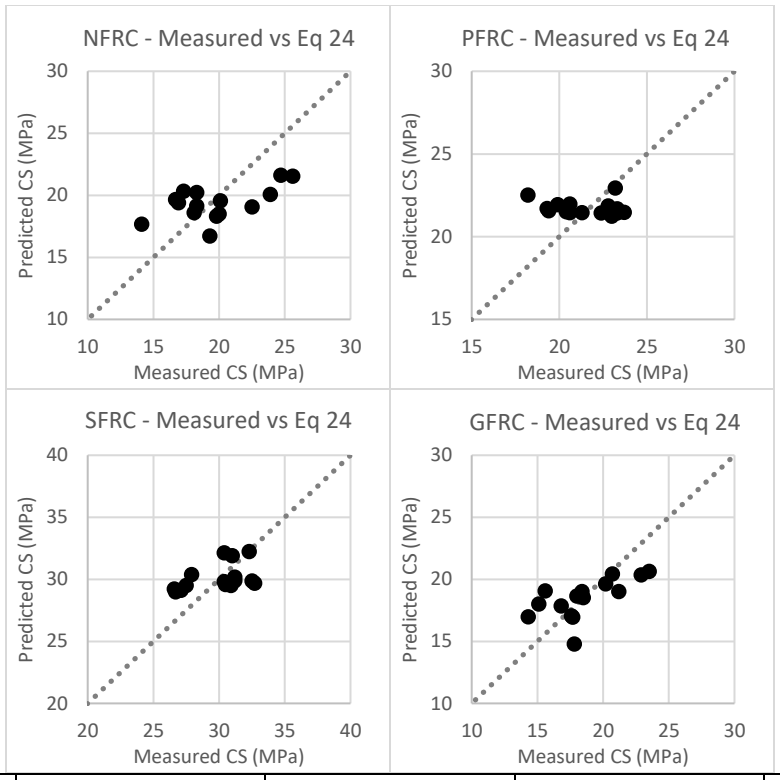

	NFRC	PFRC	SFRC	GFRC
COV	13.9%	9.1%	6.4%	11.1%

Figure 29: 3-day measured compressive strength vs proposed equation

Figure 29 compares NFRC's, PFRC's, SFRC's, and GFRC's 3-day measured compressive strength to the predicted compressive strength from equation 24. It can be observed that equation 24 obtained great results for all types of fiber reinforced concrete. Moreover, the variable "t" is set to 3 because the 3-day compressive strength is being calculated. The COV's ranged from 6.4% to 13.9% for all fiber types, fiber volume fractions, and water to cement ratios considered in this study. These results are better than those of any equation listed in Table 1.

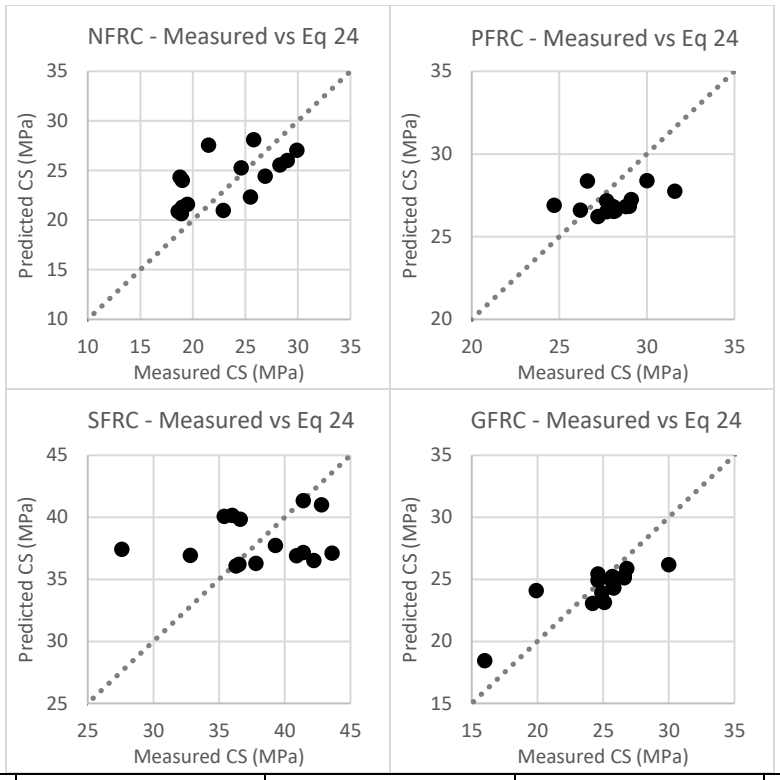

	NFRC	PFRC	SFRC	GFRC
COV	14.6%	6.6%	11.7%	8.4%

Figure 30: 7-day measured compressive strength vs proposed equation

Figure 30 compares NFRC's, PFRC's, SFRC's, and GFRC's 7-day measured compressive strength to the predicted compressive strength from equation 24. Equation 24 obtained good COV's for all types of fiber reinforced concrete in this study. Moreover, the variable "t" is set to 7 because the 7-day compressive strength is being calculated. The COV's ranged from 6.6% to 14.6% for all fiber types, fiber volume fractions and water to cement ratios considered in this study. These COV's are better than those of any equation listed in Table 1.

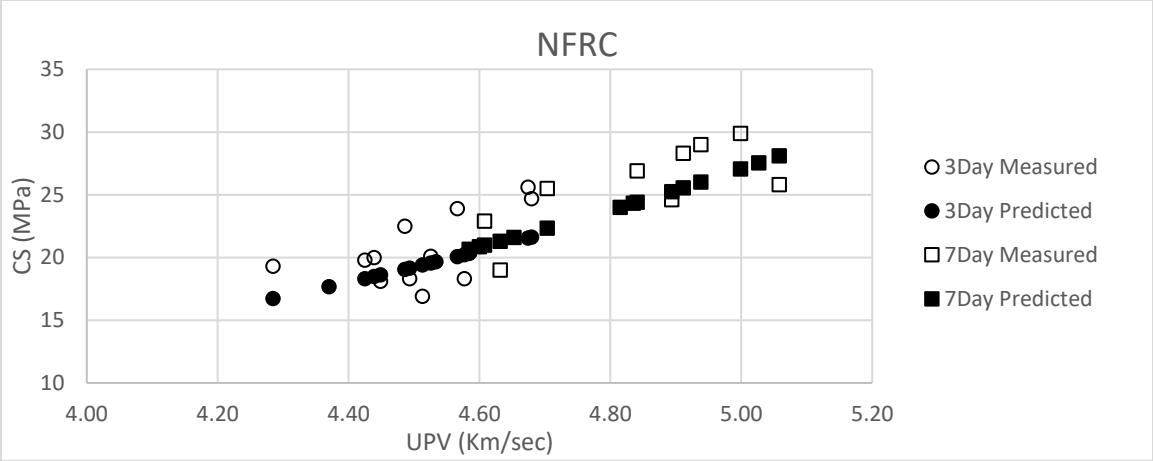

Figure 31: NFRC's 3- and 7-day compressive strength vs ultrasonic pulse velocity

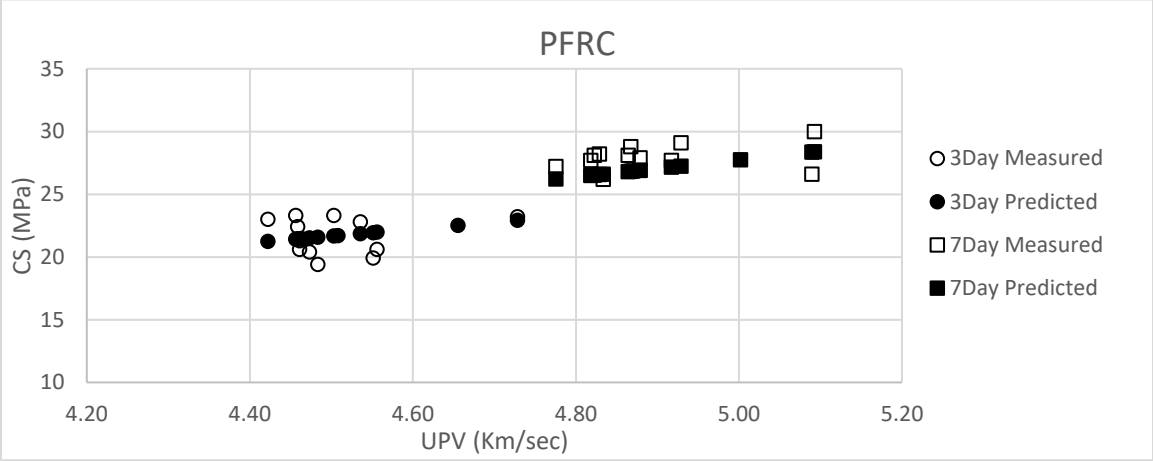

Figure 32: PFRC's 3- and 7-day compressive strength vs ultrasonic pulse velocity

Figure 31 displays the correlation between ultrasonic pulse velocity and compressive strength of all NFRC specimens at the ages of 3 and 7 days. Whereas, Figure 32 shows the correlation between ultrasonic pulse velocity and compressive strength of all PFRC specimens at the ages of 3 and 7 days. The hollow circles and squares represent the 3-day and 7-day measured data respectively and the solid circles and squares represent the 3-day and 7-day predicted compressive strength from equation 24 respectively.

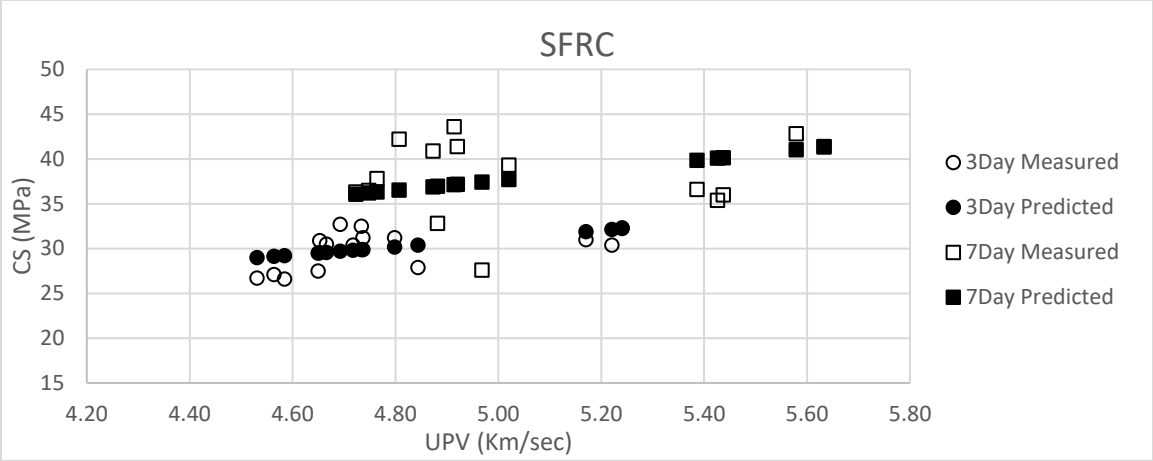

Figure 33: SFRC's 3- and 7-day compressive strength vs ultrasonic pulse velocity

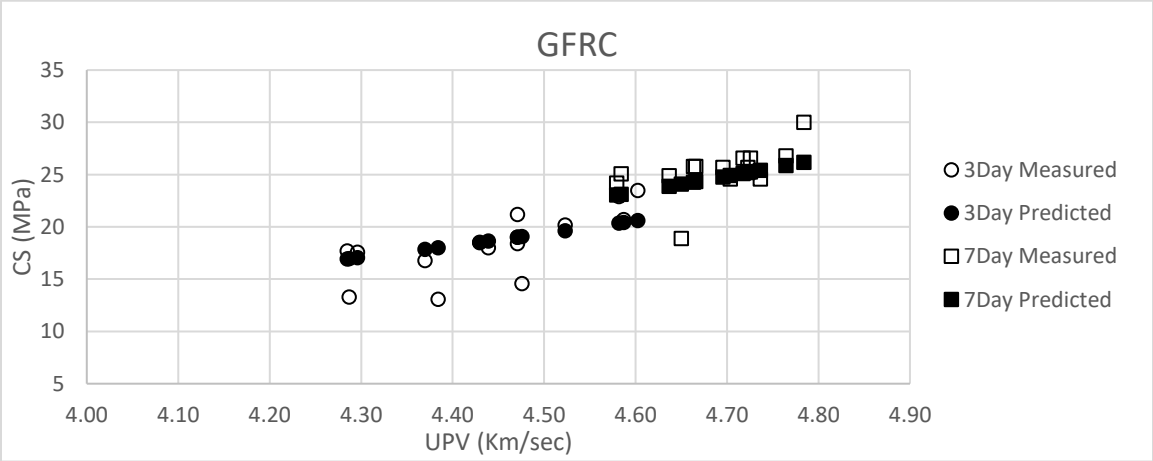

Figure 34: GFRC's 3- and 7-day compressive strength vs ultrasonic pulse velocity

Figure 33 displays the relationship between ultrasonic pulse velocity and compressive strength of all SFRC specimens at the ages of 3 and 7 days. Whereas, Figure 34 shows the relationship between ultrasonic pulse velocity and compressive strength of all GFRC specimens at the ages of 3 and 7 days. The hollow circles and squares represent the 3-day and 7-day measured data respectively and the solid circles and squares represent the 3-day and 7-day predicted compressive strength from equation 24 respectively.

The proposed equation 26 can predict the dynamic modulus of 3-day and 7-day SFRC, GFRC, PFRC, and NFRC with fiber volume fractions ranging from 0.5% vol. to 1% vol. and water to cement ratio ranging from 0.4 to 0.5. The development trend of dynamic modulus and ultrasonic pulse velocity with

hydration time is exponential at early ages (Haque and Rasel-Ul-Alam, 2018). Therefore, the prediction of FRC's early age dynamic modulus is calculated using an exponential equation. The proposed equations can predict the dynamic modulus of multiple fiber reinforced concrete types, due to the incorporation of different fiber properties as variables in the equations. No other equations have been found in the literature capable of predicting the dynamic modulus of multiple types of fiber reinforced concrete with different mixture parameters accurately. In addition, the test age is a variable in the equation making it applicable for the prediction of both 3-day or 7-day dynamic modulus. The proposed equation had good results for all types of fiber reinforced concrete considered in this study. The proposed equations for the prediction of SFRC, GFRC, PFRC, and NFRC dynamic modulus are shown below.

For G, P, and NFRC $$E_d = \alpha e^{0.46*V} \quad (26a)$$

For SFRC $$E_d = \alpha e^{0.09*V} \quad (26b)$$

Where E_d is dynamic modulus (GPa), V is the ultrasonic pulse velocity (km/sec) and α is calculated using equation 27 and fiber properties listed in Table 3. G, P, and NFRC were grouped together because they had a low density, while SFRC was left alone because it had a high density.

For G, P, and NFRC $$\alpha = 0.3\left(\frac{\sigma}{l/d}\right) + t^{0.2(\frac{\tau}{\rho})} + 2 \quad (27a)$$

For SFRC $$\alpha = 1.7\left(\frac{\sigma}{l/d}\right) + t^{4.6(\frac{\tau}{\rho})} + 2 \quad (27b)$$

Where σ is fiber flexural strength (GPa), l is fiber length, d is fiber diameter, t is the age (days), τ is fiber tensile strength (MPa), and ρ is fiber density (kg/m^3).

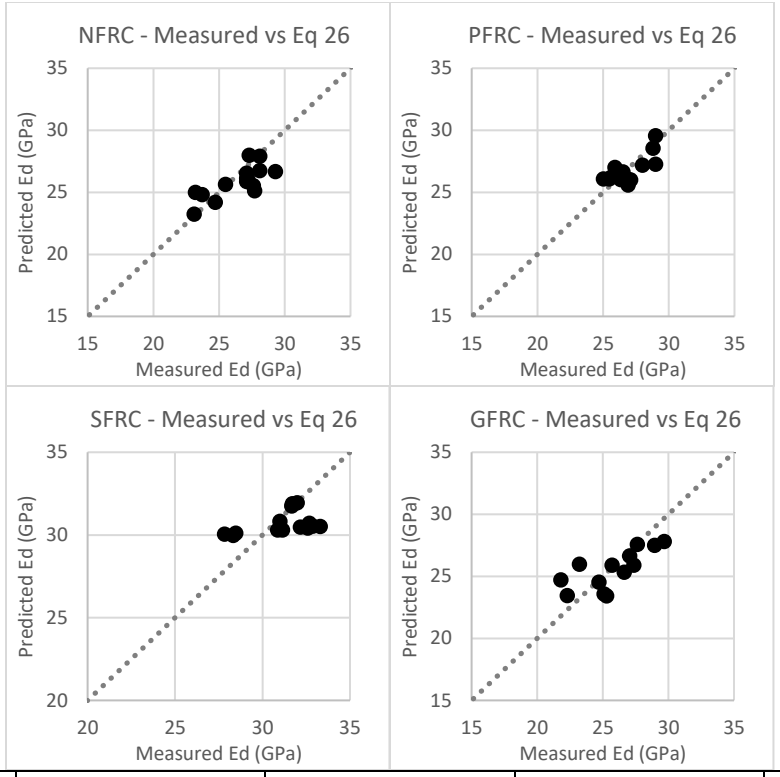

	NFRC	PFRC	SFRC	GFRC
COV	5.4%	3.3%	5.2%	9.2%

Figure 35: 3-day measured dynamic modulus vs proposed equation

Figure 35 compares the 3-day measured dynamic modulus obtained using the resonance test gauge to the predicted dynamic modulus from equation 26. The COV's are good, ranging from 3.3% to 9.2% for all fiber types, fiber volume fractions, and water to cement ratios in this study. The relationship between the resonance test gauge and ultrasonic pulse velocity is extremely good. This could be attributed to both tests being nondestructive test methods.

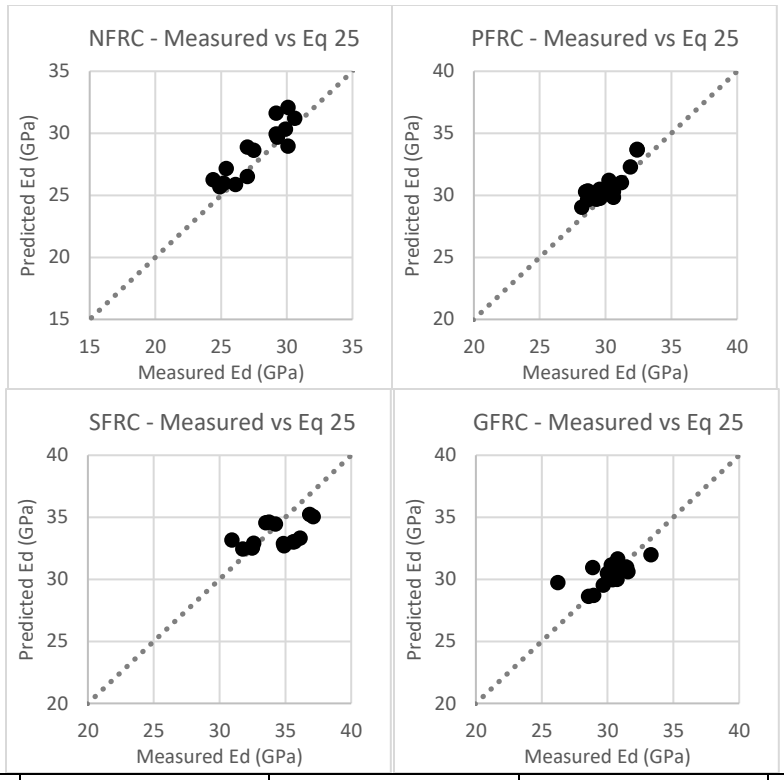

	NFRC	PFRC	SFRC	GFRC
COV	4.8%	3.3%	5.2%	9.1%

Figure 36: 7-day measured dynamic modulus vs proposed equation

Figure 36 shows the comparison between the 7-day measured dynamic modulus obtained using the resonance test gauge to the predicted dynamic modulus from equation 26. The COV's are great, ranging from 3.3% to 9.1% for all fiber types, fiber volume fractions, and water to cement ratios.

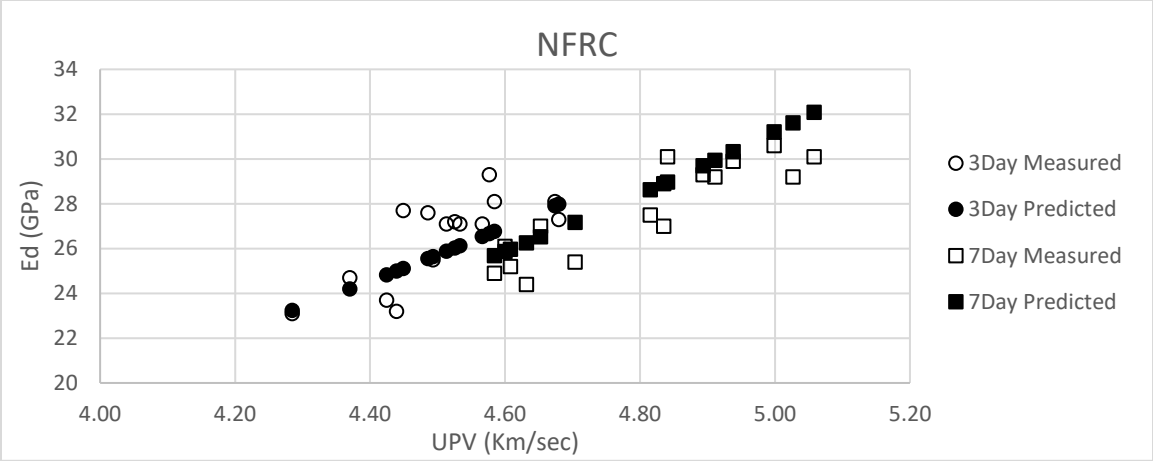

Figure 37: NFRC's 3- and 7-day dynamic modulus vs ultrasonic pulse velocity

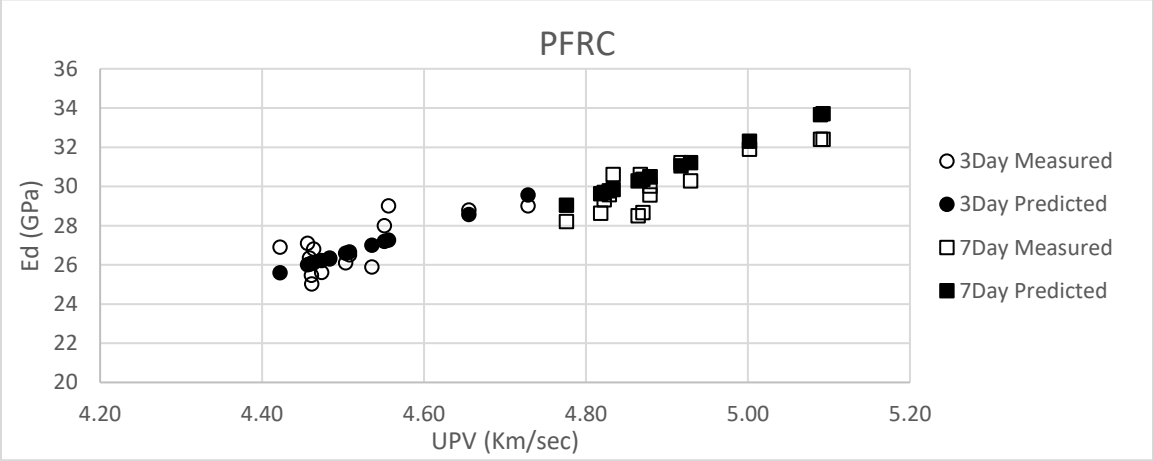

Figure 38: PFRC's 3- and 7-day dynamic modulus vs ultrasonic pulse velocity

Figure 37 shows the relationship between the ultrasonic pulse velocity and dynamic modulus of all NFRC specimens at the ages of 3 and 7 days. Figure 38 shows the relationship between the ultrasonic pulse velocity and dynamic modulus of all PFRC specimens at the ages of 3 and 7 days. The hollow circles and squares represent the 3-day and 7-day measured data respectively and the solid circles and squares represent the 3-day and 7-day predicted dynamic modulus from equation 26 respectively.

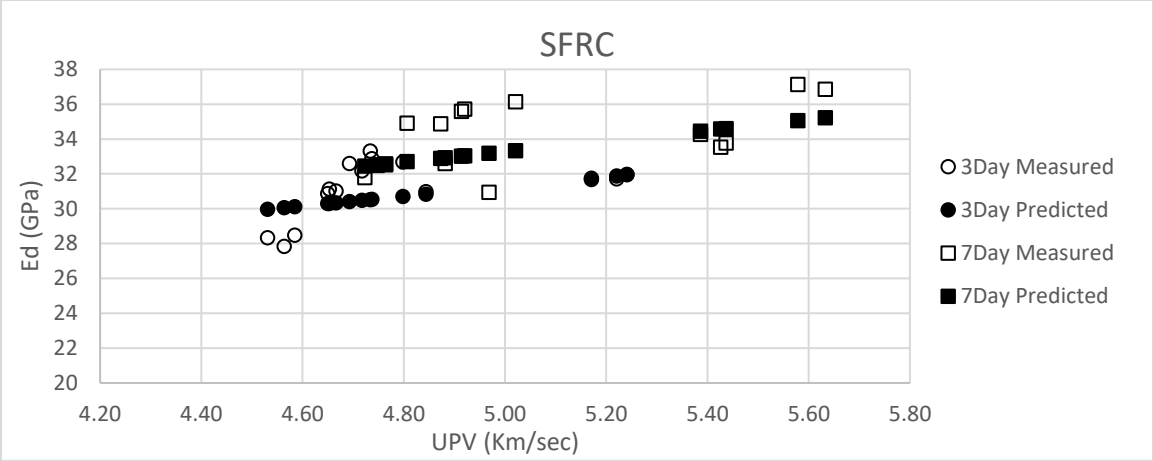

Figure 39: SFRC's 3- and 7-day dynamic modulus vs ultrasonic pulse velocity

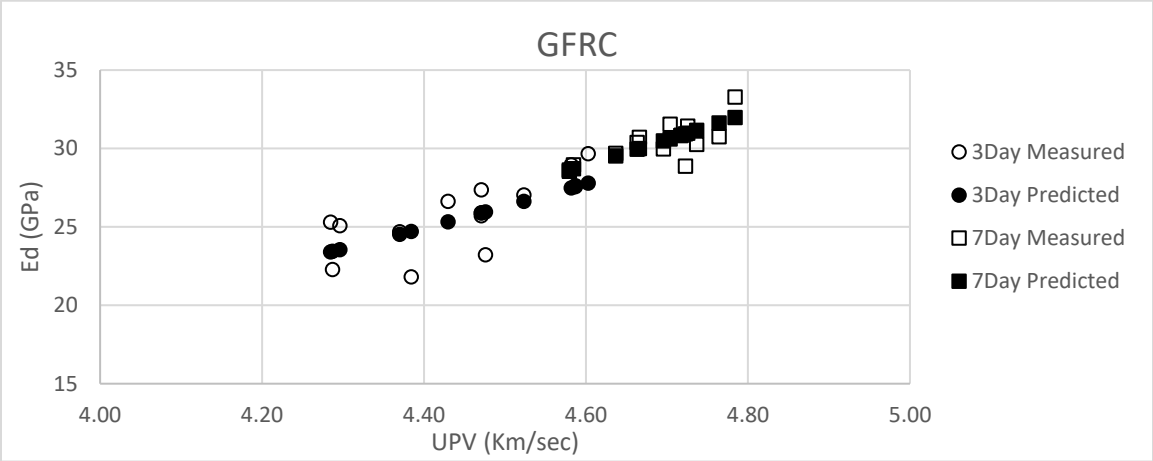

Figure 40: GFRC's 3- and 7-day dynamic modulus vs ultrasonic pulse velocity

Figure 39 shows the relationship between the ultrasonic pulse velocity and dynamic modulus of all SFRC specimens at the ages of 3 and 7 days. Figure 40 shows the relationship between the ultrasonic pulse velocity and dynamic modulus of all GFRC specimens at the ages of 3 and 7 days. The hollow circles and squares represent the 3-day and 7-day measured data respectively and the solid circles and squares represent the 3-day and 7-day predicted dynamic modulus from equation 26 respectively.

CHAPTER 5

CONCLUSION

Nondestructive testing is a wide field with a variety of options to perform quick and detailed evaluations of engineering materials. The use of nondestructive test methods to assess concrete structures is increasing mainly due to the opportunity to perform on-site assessments of existing structures accurately and without damaging the structures. The objective of the research was to predict the early age compressive strength and dynamic modulus of nylon, polypropylene, steel, and glass fiber reinforced concrete using the ultrasonic pulse velocity technique to guarantee the safety, long-term performance, and durability of fiber reinforced concrete during accelerated construction schedules. An experimental program was created to test the ultrasonic pulse velocity, dynamic modulus, and compressive strength of different types of fiber reinforced concrete. A total of one hundred eighty-nine 100 mm x 200 mm cylindrical concrete specimens were cast, cured and tested. The nylon, polypropylene, steel, and glass fibers were added independently at fiber volume fractions of 0.5% vol., 0.75% vol., and 1.0% vol. and water to cement ratios of 0.40, 0.45, and 0.50. The nondestructive and destructive testing took place after the specimens had cured in water for 1, 3, 7, and 28 days. The nondestructive tests consisted of the ultrasonic pulse velocity and the resonance test gauge, while the compression testing machine was the destructive test.

A literature review was conducted to find studies which investigated the relationship between concrete's ultrasonic pulse velocity to its compressive strength. A total of 14 equations were found in the literature relating ultrasonic pulse velocity to compressive strength taking under consideration mixture parameters such as aggregate type, aggregate content, cement type, curing temperature, water to cement ratio, shape, age, and admixtures. However, very few studies had equations that considered the effect of structural fibers on the prediction of concrete's compressive strength based on ultrasonic pulse velocity. In addition, no studies were found containing equations that specifically predicted the early age compressive strength of fiber reinforced concrete. Therefore, the accuracy of the existing equations to predict the early

age compressive strength of fiber reinforced concrete was tested by determining the coefficient of variation between the measured compressive strength to the predicted compressive strength from the existing equations. Results revealed that the existing equations didn't provided a good prediction of fiber reinforced concrete's early age compressive strength. Therefore, new empirical equations capable of predicting the early age compressive strength of FRC were created. With regards to the prediction of the dynamic modulus of concrete based on ultrasonic pulse velocity, ASTM C597 relates the ultrasonic pulse velocity of concrete to its dynamic modulus, dynamic Poisson's ratio, and density. However, determining the dynamic modulus of test specimens obtained from the field using ASTM C597's equation can be difficult because the dynamic Poisson's ratio is unknown. Therefore, new empirical equation capable of predicting the early age dynamic modulus of FRC were created.

The first proposed equation (equation 24) can predict the 3-day and 7-day compressive strength of nylon, polypropylene, steel, and glass fiber reinforced concrete with fiber volume fractions ranging from 0.5% vol. to 1.0% vol. and water to cement ratios ranging from 0.40 to 0.50. The coefficients of variation between the measured and predicted compressive strength ranged from 6.4% to 14.6%. The second proposed equation (equation 26) can predict the 3-day and 7-day dynamic modulus of nylon, polypropylene, steel, and glass fiber reinforced concrete with fiber volume fractions ranging from 0.5% vol. to 1.0% vol. and water to cement ratios ranging from 0.40 to 0.50. The coefficients of variation between the measured and predicted compressive strength ranged from 3.3% to 9.2

REFERENCES

Abdullah, M. and Jallo, E. (2011). "Mechanical Properties of Glass Fiber Reinforced Concrete". Al-Rafidain Engineering. 20(5), 128-135

Afroughsabet, V., & Ozbakkaloglu, T. 2015. Mechanical and durability properties of high strength concrete containing steel and polypropylene fibers. Construction and building materials, 94, 73-82.

Al-Nu'man, B., Aziz, B., Abdulla, S., and Khaleel, S. 2015. Compressive Strength Formula for Concrete using Ultrasonic Pulse Velocity. International Journal of Engineering Trends and Technology. 26(1), 9-13

Al-Nu'man, B., Aziz, B., Abdulla, S., and Khaleel, S. 2016. Effect of Aggregate Content on the Concrete Compressive Strength – Ultrasonic Pulse Velocity Relationship. American Journal of Civil Engineering and Architecture. 4(1), 1-5

American Concrete Institute. 2002. Report on Fiber Reinforced Concrete. ACI 544.1R-96. 38800 Country Club Drive Farmington Hills, MI 48331 USA

American Society for Testing Materials. Standard Practice for Making and Curing Concrete Test Specimens. ASTM C192. 100 Barr Harbor Drive, PO Box C700, West Conshohocken, PA 19428-2959, United States.

American Society for Testing Materials. Standard Specification for Fiber-Reinforced Concrete. ASTM C1116. 100 Barr Harbor Drive, PO Box C700, West Conshohocken, PA 19428-2959, United States.

American Society for Testing Materials. Standard Specification for Portland cement. ASTM C150. 100 Barr Harbor Drive, PO Box C700, West Conshohocken, PA 19428-2959, United States.

American Society for Testing Materials. Standard Test Method for Compressive Strength of Cylindrical Concrete Specimens. ASTM C39. 100 Barr Harbor Drive, PO Box C700, West Conshohocken, PA 19428-2959, United States.

American Society for Testing Materials. Standard Test Method for Fundamental Transverse, Longitudinal, and Torsional Frequencies of Concrete Specimens. ASTM C215. 100 Barr Harbor Drive, PO Box C700, West Conshohocken, PA 19428-2959, United States.

American Society for Testing Materials. Standard Test Method for Pulse Velocity through Concrete. ASTM C597. 100 Barr Harbor Drive, PO Box C700, West Conshohocken, PA 19428-2959, United States.

American Society for Testing Materials. Standard Test Method for Relative Density (Specific Gravity) and absorption of Coarse Aggregate. ASTM C127. 100 Barr Harbor Drive, PO Box C700, West Conshohocken, PA 19428-2959, United States.

American Society for Testing Materials. Standard Test Method for Relative Density (Specific Gravity) and Absorption of Fine Aggregate. ASTM C128. 100 Barr Harbor Drive, PO Box C700, West Conshohocken, PA 19428-2959, United States.

American Society for Testing Materials. Standard Test Method for Static Modulus of Elasticity and Poisson's ratio of concrete in compression. ASTM C469. 100 Barr Harbor Drive, PO Box C700, West Conshohocken, PA 19428-2959, United States.

Bentur, A., & Mindess, S. 2006. Fibre reinforced cementitious composites. CRC Press.

Bobde, S., Gandhe, G., and Tupe, D., 2018. Performance of glass fiber reinforced concrete. International journal of advanced research, ideas and innovations in technology, 4(3), 984-988.

British Standard Institute. 1985. Structural Use of Concrete—Part 2: Code of Practice for Special Circumstance. BS 8110-2:1995, BSI, London, UK

Dopko, M. 2018. Fiber reinforced concrete: Tailoring composite properties with discrete fibers. Graduate Theses and Dissertations. Iowa State University. Ames, IA 50011

Elvery, R. and Ibrahim L. 1976. Ultrasonic assessment of concrete strength at early ages. Magazine of Concrete Research. 28(97), 181- 90.

Fibermesh. 2016. Fiber Reinforced Concrete. 4019 Industry Drive Chattanooga, TN 37416. Engineering Report No.1603.

Gebretsadik, B. 2013. Ultrasonic Pulse Velocity Investigation of Steel Fiber Reinforced Self Compacted Concrete. UNLV Theses, Dissertations, Professional Papers, and Capstones. University of Nevada, Las Vegas.

Granju, J. L., & Balouch, S. U. (2005). Corrosion of steel fibre reinforced concrete from the cracks. Cement and Concrete Research, 35(3), 572-577.

Gul, M., Bashir, A., and Naqash, J. (2014). Study of Modulus of Elasticity of Steel Fiber Reinforced Concrete. International Journal of Engineering and Advanced Technology. 3(4),304-309

Johnston, C. D. 2001. Fiber-reinforced cements and concretes. Volume 3. CRC Press

Jones R. 1962. Nondestructive Testing of Concrete. Cambridge University Press, Cambridge

Jurowski, K. and Grzeszczyk, S. 2015. The influence of concrete composition on young's modulus. Procedia Engineering. 108(2015), 584-591

Khademi, F., Akbari, M., and Jamal S. M. 2016. Prediction of concrete compressive strength using ultrasonic pulse velocity test and artificial neural network modeling. Romanian Journal of Materials. 46(3), 343-350

Kheder, G. 1999. A two stage procedure for assessment of in situ concrete strength using combined non-destructive testing, Materials and Structures 32(6), 410-417

Kim, D. J., Park, S. H., Ryu, G. S., & Koh, K. T. 2011. Comparative flexural behavior of hybrid ultra high performance fiber reinforced concrete with different macro fibers. Construction and Building Materials, 25(11), 4144-4155.

Kolluru S. V., Popovics, J. S., and Shah, S. P. 2000. Determining Elastic Properties of Concrete Using Vibrational Resonance Frequencies of Standard Test Cylinders. Cement, Concrete, and Aggregates, CCAGDP, 22(2), 81–89.

Kosa, K., & Naaman, A. E. (1990). Corrosion of steel fiber reinforced concrete. Materials Journal, 87(1), 27-37.

Lee, G., Han, D., Han, M. C., Han, C. G., and Son, H. J. 2012. Combining polypropylene and nylon fibers to optimize fiber addition for spalling protection of high strength concrete, Construction Building

Materials, 34(2012), 313-320

Lin, Y., Kuo, S-F, Hsiao C., Lai, C-P. 2007. Investigation of Pulse Velocity- Strength Relationship of hardened Concrete. ACI Materials Journal, 104(4), 344-350

Lydon, F. D. and Balendran, R. V. 1986. Some observation on elastic properties of plain concrete. Cement and Concrete Research. 16(3), 314-324

Madhavi, T. C., Raju, L. S., and Mathur, D. 2014. Polypropylene fiber reinforced concrete – a review. International journal of emerging technology and advanced engineering. 4(4), 114-119

Mahure, N., Vijh, G., Sharma, P., Sivakumar, N., and Ratnam, M. 2011. Correlation between pulse velocity and compressive strength of concrete. International Journal of Earth Sciences and Engineering. 4(6), 871-874

Malhotra, V. M. and Carino, N. J. 2004. Handbook on nondestructive testing of concrete. CRC Press, 2 edition

Mohod M. V. (2015). Performance of Polypropylene Fiber Reinforced Concrete. IOSR Journal of Mechanical and Civil Engineering. 12(1), 28-36

Naaman, A. E. 2003. Engineered steel fibers with optimal properties for reinforcement of cement composites. Journal of advanced concrete technology, 1(3), 241-252.

Naik, T., Malhotra, V., and Popovics, J. 2004. The Ultrasonic Pulse Velocity Method, Chapter 8. CRC Press

Nash't, I., A'bour, S., and Sadoon, A. 2005. Finding an unified relationship between crushing strength of concrete and non-destructive tests. 3rd MENDT, Middle East Nondestructive Testing Conference & Exhibition, Bahrain, Manama

Nehdi, M. L. and Soliman, A. M. 2011. Early-age properties of concrete: Overview of fundamental concepts and state-of-the art research. Construction Materials. 164(2), 57-77

Neville, A. M. 2004. Properties of concrete, 4th edn. Wiley Harlow, New York, USA

Nitin and Verma, S., 2016. Effect on Mechanical Properties of Concrete Using Nylon Fibers. International Research Journal of Engineering and Technology, 3(7), 1751-1755.

Nycon. 2020. Nylon fibers. 300 Ben Fairless Drive Fairless Hills, PA 19030

Ozsar, D. S., Ozalp, F., Yilmaz, H. D., and Akcay, B. 2017. Effect of nylon fiber and concrete strength on the shrinkage and fracture behavior of fibre reinforced concrete. Strain-Hardening Cement Based Composites. Springer, Dordrecht, RILEM Bookseries, Vol 15, 188-194.

Pane, I. and Hansen, W. 2002. Early-age creep and stress relaxation of concrete containing blended cements. Materials and Structures Journal. 35(2), 92-96

Patel, P. A., Desai, A. K., and Desai, J. A. 2012. Evaluation of engineering properties for polypropylene fiber reinforced concrete. International Journal of Advanced Engineering Technology. 3(1), 42-45

Pawade, P., Nagarnaik, P., and Pande, A. (2011). Performance of steel fiber on standard strength concrete in compression. International Journal of Civil and Structural Engineering. 2(2), 483-492

Popovics, S., Rose, J., and Popovics, J. (1990). The behaviour of ultrasonic pulses in concrete. Cement and Concrete Research. 20(2), 259-270

Qureshi, L. A. and Ahmed, A. 2013. An investigation on strength properties of glass fiber reinforced concrete. International Journal of Engineering Research and Technology. 2(4), 2567-2572

Ramli M. and Hoe K. (2010). Influences of Short Discrete Fibers in High Strength Concrete with very Coarse Sand. American Journal of Applied Sciences. 7(12), 1572-1578

Raouf, Z. and Ali, Z. 1983. Assessment of Concrete Characteristics at an Early Age by Ultrasonic Pulse Velocity. Journal of Building Research. 2(1), 31-44

Shanya, O., Daiki, U., Hiroshi, Y., and Katsufumi, H. 2016. Effectiveness of recycled nylon fibers as reinforcing material in mortar. Journal of Asian Concrete Federation. 2(2), 102-109

Song, P. S. and Hwang, S. 2004. Mechanical propertied of high-strength steel fiber reinforced concrete. Construction and Building Materials. 18(9), 669-673.

Song, P. S., Hwang, S., and Sheu, B. C. 2015. Strength properties of nylon and polypropylene fiber reinforced concretes. Cement and concrete research. 35(8), 1546-1550

Soulioti, D. V., Barkoula, N. M., Paipetis, A., & Matikas, T. E. 2011. Effects of Fibre Geometry and Volume Fraction on the Flexural Behaviour of Steel‐Fibre Reinforced Concrete. Strain. 47(1), 535-541

Spadea, S., Farina, I., Carrafiello, A., and Fraternali, F. 2015. Recycled nylon fibers as cement mortar reinforcement. Construction and Building Materials. 80(2015), 200-209

Subramanian, E. S., Vaishnave, V. R., and Vignesh, V. T. S. 2016. Experimental Investigation of concrete composite using nylon fiber. International Journal of Engineering Sciences and Research Technology. 5(12), 998-1002

Suksawang, N., Wtaife, S., and Alsabbagh, A. 2018. Evaluation of Elastic Modulus of Fiber Reinforced Concrete. ACI Materials Journal. 115(2), 239-249

Tharun, A., Pushpan, A., Anjitha U., Johnson, J., Thomas, M., Priya, P., and Shifa, K. 2018. Experimental Investigation on Strength Properties of Nylon Fiber Reinforced Concrete Pavements. International Journal of Engineering Research and Technology 6(6), 1-6

Thirumurugan, S. and Kumar, S. A. 2013. Compressive Strength Index of crimped polypropylene fibers in high strength cementitious matrix. World applied sciences journal. 24(6), 698-702

Verma, S. K., Bhadauria, S. S., and Akhtar, S. 2013. Review of Nondestructive Testing Methods for Condition Monitoring of Cwoncrete Structures. Journal of Construction Engineering. 1(2013), 1-11

Wiciak, P., Cascante G., and Polak, M. A. 2017. Sensor and dimension effects in ultrasonic pulse velocity measurements in mortar specimens. Procedia Engineering. 193(2017), 409-416

Wu, G., Wang, X., Wu, Z., Dong, Z., & Zhang, G. 2015. Durability of basalt fibers and composites in corrosive environments. Journal of Composite Materials, 49(7), 873-887.

Yang E., Wang S., Yang Y., and Li V. (2008). Fiber-Bridging Constitutive Law of Engineered Cementitious Composites. Journal of Advanced Concrete Technology. 6(1), 181-193

Ye, G., Lura, P., Van Breugel, K., and Fraaij, A. L. 2004. Study on the development of the microstructure

in cement-based materials by means of numerical simulation and ultrasonic pulse velocity measurement. Cement and Concrete Composites, 26(5), 491-497

Yin, S., Tuladhar, R., Collister, T., Combe, M., Sivakugan, N., and Deng, Z. 2015. Post-cracking performance of recycled polypropylene fiber in concrete. Construction and Building Materials, 101, 1067-1077

Yin, S., Tuladhar, R., Riella, J., Chung, D., Collister, T., Combe, M., & Sivakugan, N. 2016. Comparative evaluation of virgin and recycled polypropylene fibre reinforced concrete. Construction and Building Materials, 114, 134-141.

Yoon, H., Kim, Y., Kim, H., Kang, J., and Koh, H. 2017. Evaluation of Early-Age Concrete Compressive Strength with Ultrasonic Sensors. Sensors. 17(8): 1-15.

Zheng, Y., Wu, X., He, G., Shang, Q., Xu, J., and Sun, Y. 2018. Mechanical Properties of Steel Fiber Reinforced Concrete by Vibratory Mixing Technology. Advances in Civil Engineering. 2018, 1-11

Haque, M. I. and Rasel-Ul-Alam, Md. (2018). "Non-linear models for the prediction of specified design strengths of concretes development profile". HBRC Journal. 14(2), 12

APPENDIX A

APPENDIX B